STORM GENERATED, EPISODIC SEDIMENT MOVEMENTS OFF KAHE POINT, OAHU, HAWAII

A THESIS SUBMITTED TO THE GRADUATE DIVISION OF THE UNIVERSITY OF HAWAII IN PARTIAL FULFILLMENT OF THE REQUIREMENTS FOR THE DEGREE OF

MASTER OF SCIENCE

IN GEOLOGY AND GEOPHYSICS

DECEMBER 1985

By

Bruce Osamu Tsutsui

Thesis Committee:

William T. Coulbourn, Chairman
John F. Campbell
Ralph Moberly

We certify that we have read this thesis and that, in our opinion, it is satisfactory in scope and quality as a thesis for the degree of Master of Science in Geology and Geophysics

THESIS COMMITTEE

_____

Chairman

_____

_____

ACKNOWLEDGMENTS

Although this document bears my name, I am indebted to many other people who put in their time and efforts. The project was partially funded by Dr. Patrick Takahashi of the Hawaii Natural Energy Institute. Dr. Richard Young provided ship time for coring operations. I wish to thank Dr. Edward Noda, Dr. Charles Hollister, Dr. Daniel Fornari, Dr. Frans Gerritsen, Dr. Eric DeCarlo and Mr. Bob Pittman for contributed data, ideas and advice.

I wish to express special thanks to Dr. Johanna Resig for her help in foraminiferal identification and zonations. Dr. Jane Schoonmaker provided lab space, equipment and sat on the thesis defense committee.To Dr. Fritz Theyer, I would like to express gratitude for all his help in the early stages of my M.S. I would also like to extend special thanks to my committee members; to Mr. J.F. Campbell, who was the direct or indirect source for the bulk of my data; to Dr. Ralph Moberly, for providing so many insights on the study area; and to my advisor, Dr. William Coulbourn, for his advice, patience, humor and skill in getting me through the many crises which occurred during the course of this project.

Most of all, I would like to thank my parents for getting me here in the first place; and to Ms. Sharon Parker, for expert cartographic advice, for moral support and for putting up with my innumerable mood swings during this project.

ABSTRACT

The area off Kahe Point, Oahu, Hawaii is the focus of recent oceanographic research in preparation for this nation's first large-scale Ocean Thermal Energy Conversion (OTEC) Project. Underwater instrument arrays moored to the bottom in this area were damaged, shifted or lost during the passage of Hurricane Iwa in 1982. Five underwater telephone cables located at greater depths were severed during the same period.

Images produced from SeaMARC II survey of the seafloor reveal that most of the bottom is represented by a background of light tones interpreted as smooth sediment cover. Cores collected from these areas contain thick sequences of hemipelagic silt and clay-sized material. These areas are interrupted by dark tones interpreted as downslope trending patterns of rough bottom. Cores from the areas represented by the dark tones contain coarse sands and displaced shallow benthic foraminifera. The pattern configurations and sediment types indicate that the darker tones represent downslope sediment flow. The locations of these patterns correspond to the positions of the underwater cable damage and displacements of instrument arrays which occurred during the passage of Hurricane Iwa.

The evidence indicates that hurricane-generated sediment movement caused the damages and displacements. Recurrence of these movements pose potential hazards to a large cold-water intake pipe to be built in this area as part of the OTEC project.

TABLE OF CONTENTS

Page

LIST OF TABLES

LIST OF FIGURES

PURPOSE OF STUDY

The objective of this study is to describe the ocean bottom off Kahe Point, Oahu, Hawaii (Fig. 1) with special emphasis on the character and episodic movements of the surficial sediment cover. Assessment of the nature of the ocean bottom and its stability is of importance to planned construction of a large natural-energy project at Kahe Point. Whereas this study is primarily geologically oriented, the information contained within may be of potential value to engineers and planners.

INTRODUCTION

Background

The Kahe Point area is the focus of recent oceanographic research done under the auspices of the United States Department of Energy (DOE) in preparation for this nation's first commercial scale Ocean Thermal Energy Conversion (OTEC) generator (Yuen, 1981). One study (Noda, 1983) monitored the local oceanic thermal gradient utilizing an array of underwater current, temperature and pressure sensors moored to the

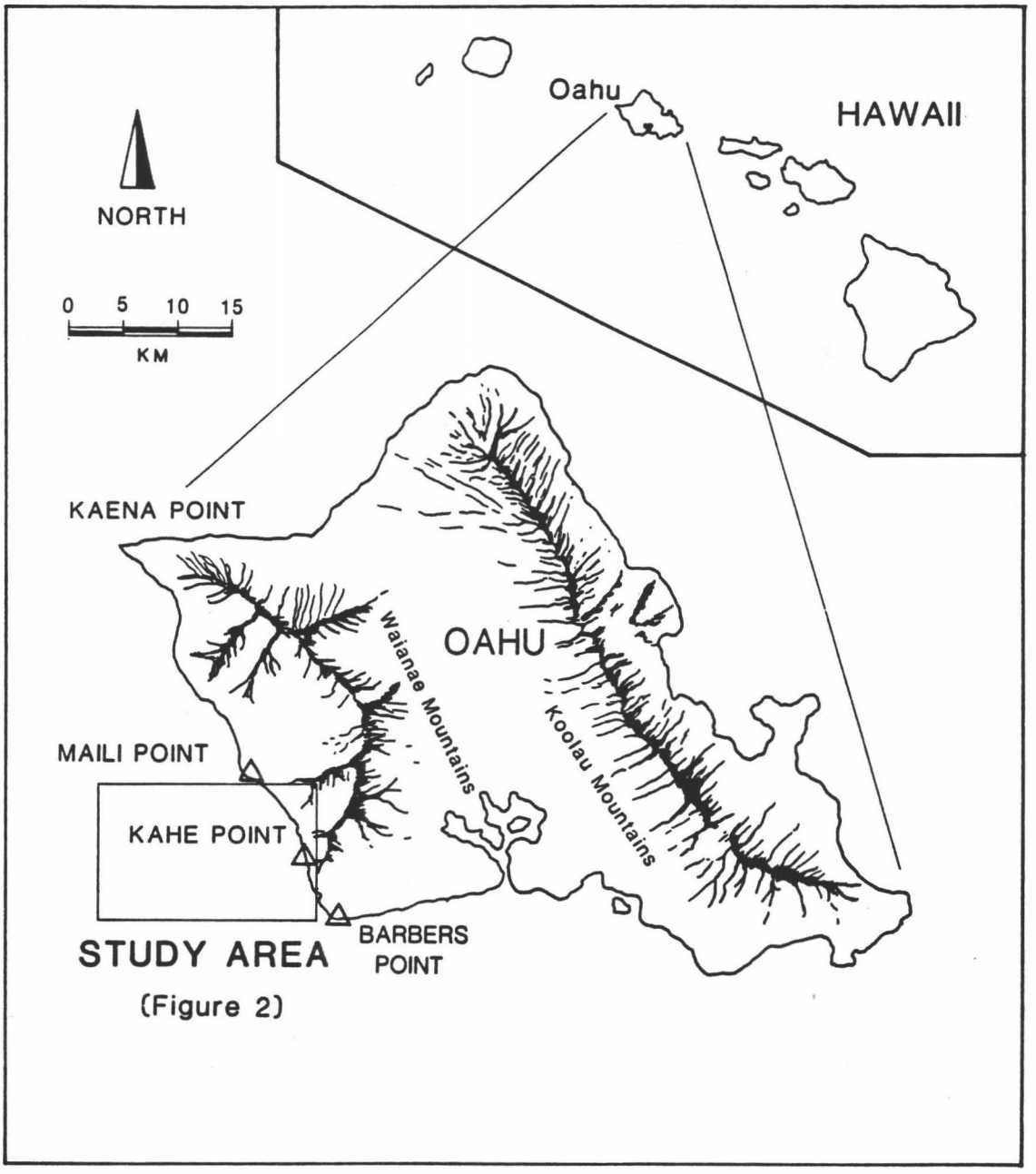

Figure 1. Study area location map. Triangles locate navigational beacon stations. Rectangular inset enlarged in Figure 2.

ocean bottom at several locations off Kahe Point. During late November, 1982, these sensors were shifted, damaged or lost as a result of the passage of Hurricane Iwa near the Hawaiian Islands. During the same period, four underwater telephone cables located in deeper areas farther offshore Kahe Point and two located off Kaena Point, Oahu, were damaged or severed. Evidence from the study area indicates that displacement of ocean bottom sediment, occurring as a result of the hurricane, was responsible for both the underwater cable damage and the movement of the instrument arrays.

These circumstances provide a unique opportunity to study underwater sedimentary processes; in particular short term, episodic events. In addition to providing an interesting focus for academic study, this research is important from an engineering and planning viewpoint. The cold-water intake pipe planned for the Kahe Point OTEC generator will be 10 m (33 ft) in diameter, will extend to a depth of approximately 700 m (2210 ft) and will span a distance of about 1.5 km (0.9 miles) from shore. The importance of stable substrate to structures of this size mandates a careful assessment of possible risk.

Geologic Setting

The study area is located off the Waianae coast, southwest Oahu, and consists of an underwater shelf and slope extending approximately 1 to 2.5 km from shore between Kahe Point and Maili Point (Figs. 1 and 2). Because rainfall on Oahu is primarily orographic, the Waianae coastline is relatively arid. Streams along this section of coastline

Figure 2. Bathymetry and sediment cover, Kahe Point study area (after Normark et al., 1982). Line patterns indicate irregular seismic reflectors, shaded pattern indicates distinct planar or wavy continuous reflectors. Dot patterns show locations of sand wedges along the shelf (after Campbell et al., 1970; Noda, 1983 and Coles, 1984). Box outline locates Figure 3.

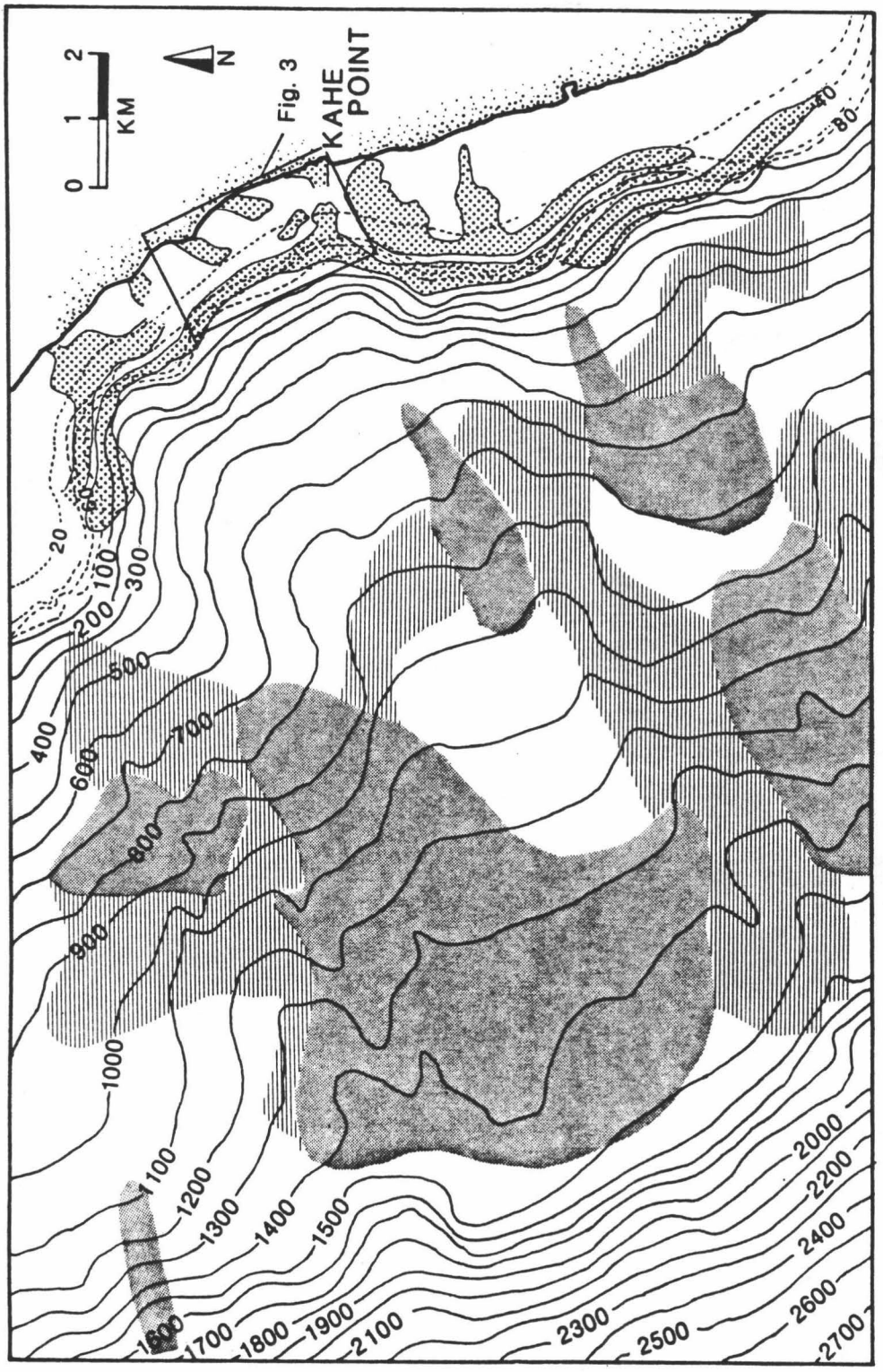
0 1 2
KM
N
Fig. 3
KAHE
POINT
20
60
100
200
300
400
500
600
700
800
900
1000
1100
1200
1300
1400
1500
1600
1700
1800
1900
2100
2300
2500
2600
2700
40
80

are intermittent, with flow and sediment discharge into the offshore environment occurring only after infrequent storms (Maragos, 1979; Macdonald et al., 1983).

Extensive volcanism terminating about 2.7 million years ago constructed the volcanic bedrock making up the underwater slope of this coastline (Macdonald et al., 1983). A long period of quiescence and extensive erosion followed, during which the large valleys dominating the present coastal geomorphology were formed (Macdonald et al., 1983).

The bathymetric contours of the study area roughly resemble the configurations of neighboring Lualualei, Kahe and Nanakuli valleys, implying a general relationship between terrestrial and marine drainage systems. Subaerial valley walls elsewhere around Oahu connect with walls of adjoining submarine canyons buried beneath layers of young sediment cover and reef (Coulbourn et. al., 1974). Subaerial erosion, isostatic subsidence, eustatic sea-level changes and concurrent filling of valleys by fluvial and shallow marine sediments are the most probable explanations for the submarine morphology offshore of Kahe Point. Borehole drillings in Lualualei Valley penetrated up to 360 m (1200 ft) of interbedded alluvial and shallow marine sediment (Stearns, 1935). Resig (1969) also outlined several cycles of marine transgression and regression using foraminiferal populations within sediment samples from two long drill cores collected from the nearby Ewa Plain.

Most of the marine research focusing on the underwater area off the southwest Waianae coast has been done in connection with the building and operation of the Hawaiian Electric Company (HECO)

generating plant (Fig. 3). Since the beginning of operations in 1963, HECO environmental monitoring has centered mainly on the effects of a warm-water outfall on local nearshore coral reefs and on beach-sand circulation (Marine Advisors, 1964; URS, 1973; Coles, 1979). Brock and Chamberlain (1967) conducted a survey of the shelf north of Maili Point using a submersible and geophysical methods; these dives revealed structures similar to those surveyed in the Kahe Point area. Campbell et al. (1970) traversed the entire Waianae coastline as part of a larger study of sand deposits located on the shallow underwater shelf paralleling leeward Oahu. Since the advent of the Kahe Point OTEC project, several detailed studies of the deeper offshore areas have been conducted utilizing 3.5 kHz seismic reflection profiling, SeaMARC II side-scan sonar mapping, sediment sampling, submersible dives and ocean bottom photography (Coles, 1982; Normark et al., 1982; Noda, 1982, 1983; Fornari, 1983, 1984; Hollister, 1984).

Bathymetry of the study area (Normark et al., 1982) reveals a narrow shelf, a steep escarpment and a moderate slope (Fig. 2). From shore the shelf inclines gently seaward at about 4^{o} to 5^{o} to depths of roughly 100 to 110 m (330 to 360 ft). This shelf is divided into two sections, the first extending from shore to a prominent riser between 50 to 70 m (165 to 232 ft) depth. This depth range correlates well with depths representative of the Penguin Bank submerged shoreline (Stearns, 1974; Macdonald et al., 1975). The second portion of the shelf continues seaward from the foot of the Penguin Bank step and terminates at about 110 m (330 ft) depth in a prominent escarpment

whose edge corresponds to the Mamala-Kahipa stand of the sea (Coulbourn et al., 1974; Stearns, 1974; and Fornari, 1983). The distance from shore to the edge of this shelf varies, ranging from 1 to 2.5 km. Stearns (1974) asserts that the Mamala-Kahipa shelf-edge marks the last major low-stand of the sea, corresponding to an age of approximately 12,000 years b.p.

The thickness of the sediment cover from shore to shelf-edge varies. The shoreline is composed of a raised reef platform interrupted by three separate beaches (Fig. 3). Survey done for HECO indicates that most of the nearshore areas consist of submerged reef platform, cut by several sand-filled channels connecting to the beaches (Marine Advisors, 1964). The HECO surveys and environmental monitoring indicate that sand circulation is predominantly longshore, with net transport to the south, and that a portion of the annual sand circulation is lost to deeper areas (Coles, 1979).

Seismic reflection surveys of the shelf off Kahe Point revealed a sand wedge 5 to 17 m (17 to 55 ft) in thickness located along the shelf-break (Noda, 1982). The thickest deposits were found between the base of the the 50 to 70 m step and the edge of the shelf. Sand-filled channels connect shelf-edge wedges to beaches along the entire study area (Fig. 2). The largest and thickest accumulations of sediment occur just south of Maili Point and off Kahe Point. Observers on submersible dives reported sand-filled channels in the vicinity of Kahe Point (Coles, 1982). These channels resemble others surveyed to the north of the study area and "river-like" masses of sand more than 30 m

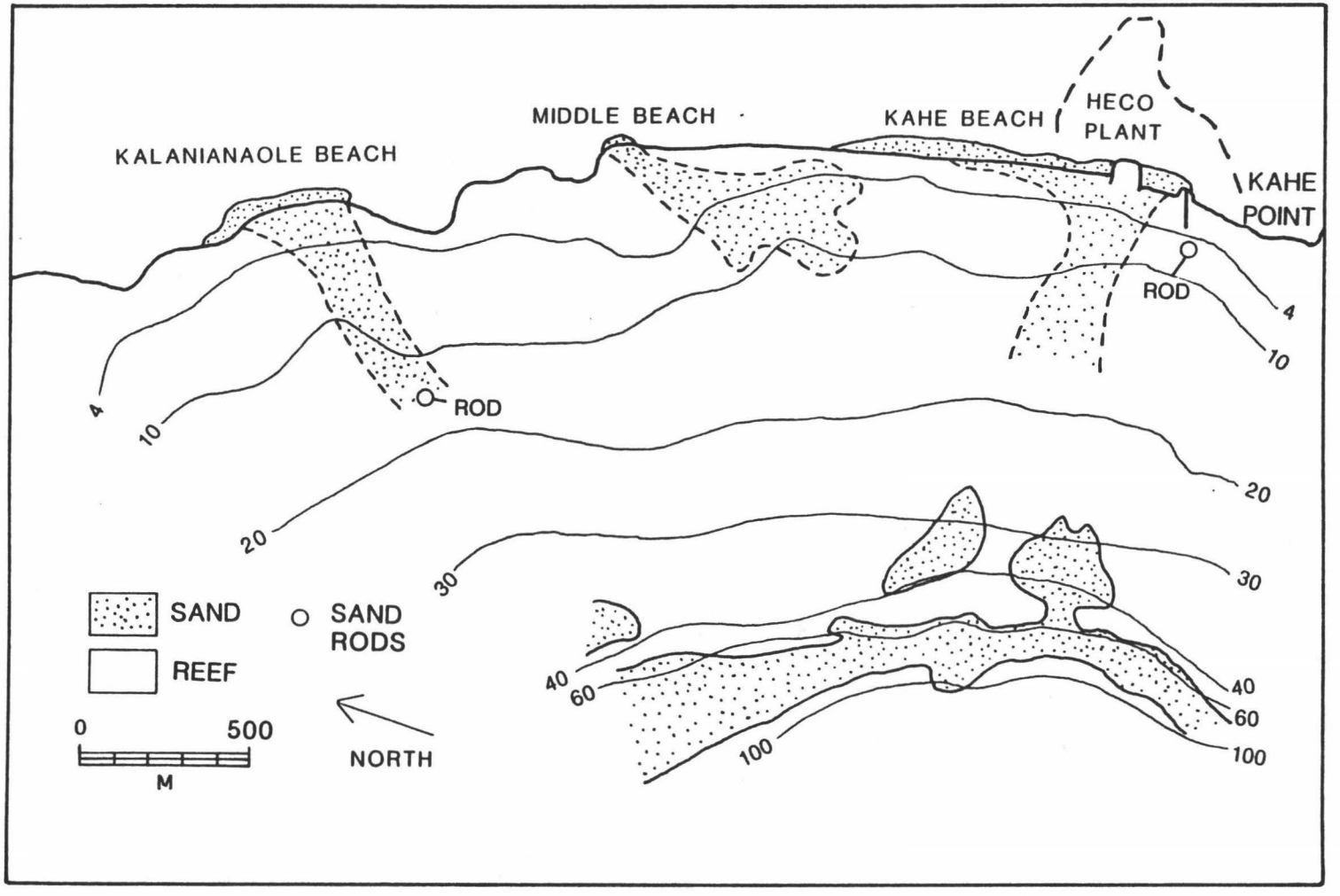

Figure 3. Beaches, sand-filled channels, sand wedges and location of measuring rods remaining in the Kahe Point area after the passage of Hurricane Iwa (after Noda, 1983 and Coles, 1984).

in width covering both the Mamala (Mamala-Kahipa in this study) and Penguin Bank shelves off Kaena Point (Brock and Chamberlain, 1967).

Beyond the shelf-break, depth increases rapidly along an escarpment down to a depth of about 300 to 350 m (990 to 1200 ft), approximately the depth of the Lualualei shoreline (Macdonald et al., 1983). The slope averages about 30° to 40°, but approaches 90° along parts of the escarpment. Observed from a submersible, its face is a "variably karstified carbonate slope with across-slope microtopographic relief of between 0.25 and 0.50 m " (page 8, Fornari, 1983). Below the 300 m depth contour marking the approximate base of the escarpment, slope angles gradually decrease, averaging about 10° to 20°. At a depth of about 1500 m (4800 ft) slope angles increase to approximately 30° representing the original submarine slope of the Waianae Volcano (Campbell, 1985, pers. comm). A conspicuous rectangular re-entrant cuts into the face of the escarpment. A noticeable bulge in the depth contours downslope from this feature may mark an accumulation of slumped sediment and rock (Fig. 2). This configuration indicates that the re-entrant is perhaps a detachment surface. Because of the relatively large size of this feature (approximately 1 to 2 km across), the slump may include volcanic bedrock (Normark et al., 1982). Slumping of bedrock was invoked to explain bathymetric configurations off portions of Oahu and other Hawaiian submarine slopes (Moore, 1964; Fornari, 1982; Fornari and Campbell, in press). Alternatively, the re-entrant may mark a constructional feature. Subaerial erosion of a large valley and subsequent transgression of the ocean would result in

the building of fringing and patch reefs which could form the present re-entrant configuration. The sides of this submerged valley re-entrant may then have served as a large channel, directing subsequent downslope movement of sediment, and creating the bulge in contours.

Observations during submersible dives off Kahe Point gave no signs of fresh breaks on the escarpment face, nor other signs of recent bedrock movement (Fornari, 1983). Samples collected from the base of this escarpment yielded Carbon-14 ages of about 20,000 years (Fornari, 1983). This apparent stability indicates that the slump is not a product of substrate movement within the last few years, and is not responsible for movements and damage which occurred during the passage of Hurricane Iwa.

Beyond the base of the escarpment, reflections displayed on 3.5 and 12 kHz seismic profiles range from discontinuous--disordered sediment or rock, to continuous--smooth sediment mantled sea-floor, to acoustically transparent--structureless or disordered sediment. According to Normark et al. (1982). The areal distribution of reflectors indicating disordered or structureless sediment may delineate areas of sliding or mass movement (Fig. 2).

EFFECTS OF HURRICANE IWA

Attributes of the Storm

On 23 November 1982, Hurricane Iwa, the most destructive storm in the recorded history of Hawaii, passed near the islands of Niihau and Kauai, causing damage estimated at more than 400 million dollars (Chiu et al., 1983; Noda, 1983). Hindcast reconstruction of the characteristics of Hurricane Iwa reveals several attributes which distinguish this storm from the more typical hurricane passing through the Hawaiian area. Iwa's appearance in late November was after the normal hurricane season of July to September. Iwa was tracked at a speed of about 20 knots, approximately two to three times the normal, and also showed a general southwest to northeast path instead of the more typical east to west approach (Noda, 1983).

The best track shows that the eye of the hurricane passed near Kauai and the weather station at the Pacific Missile Range, Barking Sands (PMRBS), about 150 km west of Kahe Point (Fig. 4). Recordings at PMRBS showed sustained wind speeds of 50 to 70 knots with gusts of up to 81 knots. At Barbers Point, Oahu (5 km south of Kahe Point) and at Honolulu International Airport (12 km southwest of Kahe Point) sustained wind speeds were 30 to 35 knots and gusts reached 64 knots (Noda, 1983).

Direct measurements of wind and wave conditions for the Kahe Point area are not available, but can be reconstructed based on a model for calculating wind and wave conditions with distance from the center of a

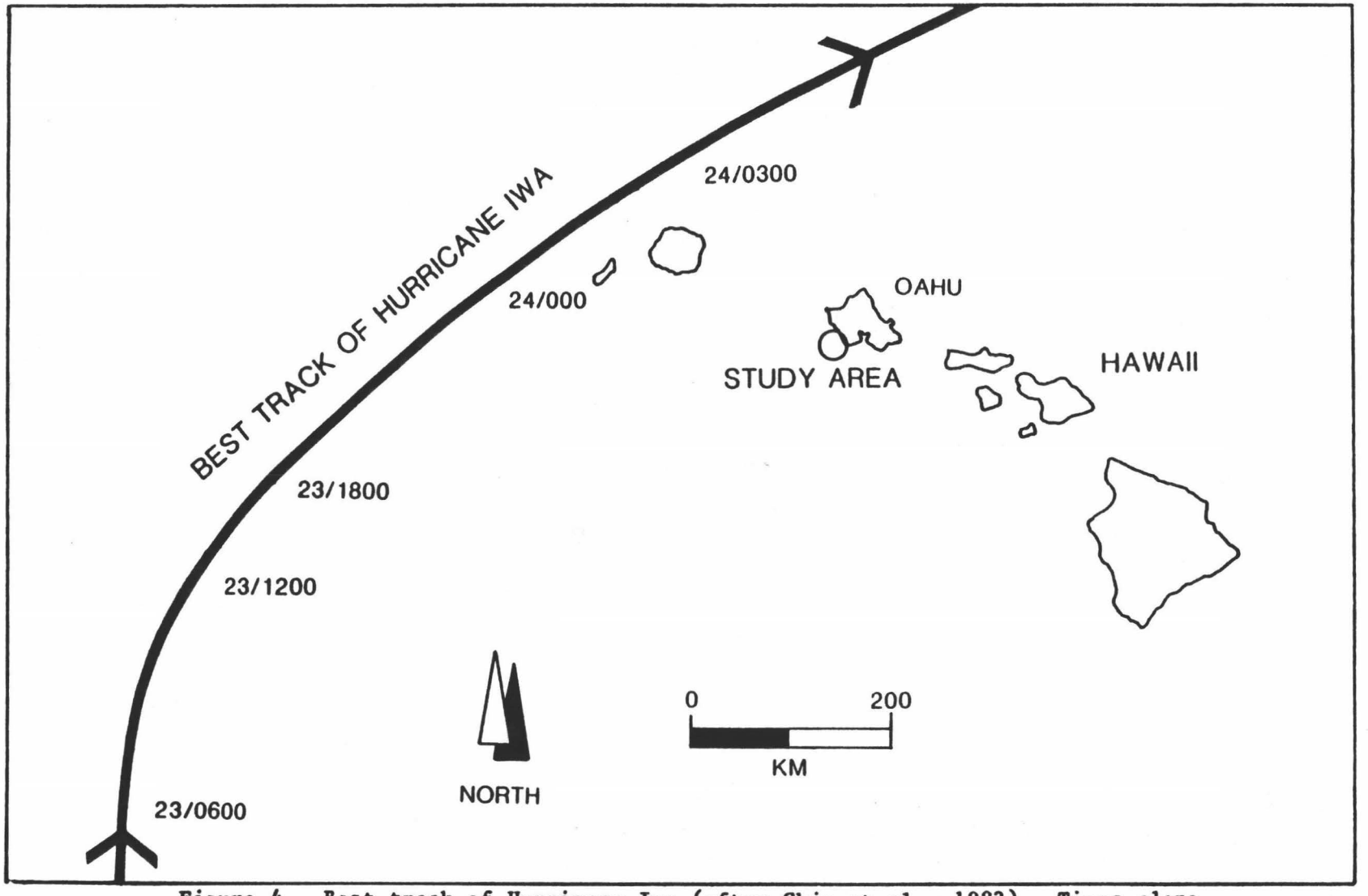

Figure 4. Best track of Hurricane Iwa (after Chiu et al., 1983). Times along track are Greenwich Mean Time (GMT) for November 23 and 24, 1982.

100 year hurricane event (Bretschneider, 1980). Using this model, Noda (1983) computed a significant wave height (the average of the highest third of all wave height measurements) of about 5 m (16.5 ft), a maximum wave height of approximately 9 m (30 ft) and sustained winds of 30 to 35 knots. The calculation incorporated available data from PMRBS, Barbers Point and Honolulu International Airport.

Underwater Telephone Cable Damage and Breaks

During the passage of Hurricane Iwa, the Hawaiian Telephone Company experienced successive disruptions of service through cables located off the Waianae Coast. The outages of communication occurred within a relatively short span of time, but because of intense activity involved in immediate switching of service to alternate routes, determinations of outage times by company personnel were approximate (Table 1).

Approximate locations of cable positions, breaks, and irretrievable sections of cable thought to be buried are shown on Figure 5. Positions of damage were estimated by grappling from both sides of a damaged section of cable and metering distances to breaks as cable was reeled onto the cable laying ship C/S Enterprise. Increases of cable tension during grappling indicate that cable sections were probably buried under sediment, and some of these recovered sections displayed abrasions on their outer casings. In several instances during recovery operations, the tensile strength of cables was exceeded, and they parted (Noda, 1983; Hollister, 1984).

Table 1

Submarine Cable Descriptions and Estimated Outage Times on November 23, 1982

Cable No.	System/Description	Estimated Time of Outage (HST)	Remarks
1	Hanauma Bay-Makaha Tie Cable (Hawaiian Telephone Co./AT&T)	1925	Broken
2	San Luis Obispo, CA-Makaha (Hawaiian Telephone Co./AT&T)	1950	Broken
3	Guam-Makaha (Hawaiian Telephone Co./AT&T)	1920	Damaged But Usable
4	Johnston Island-Makua (Military)	1920	Damaged
5	New Zealand-Keawaula (Compac)	1920	Damaged*
6	Vancouver-Keawaula (Compac)	1920	Broken*

* Damage locations off Kaena Point

(From Noda, 1983)

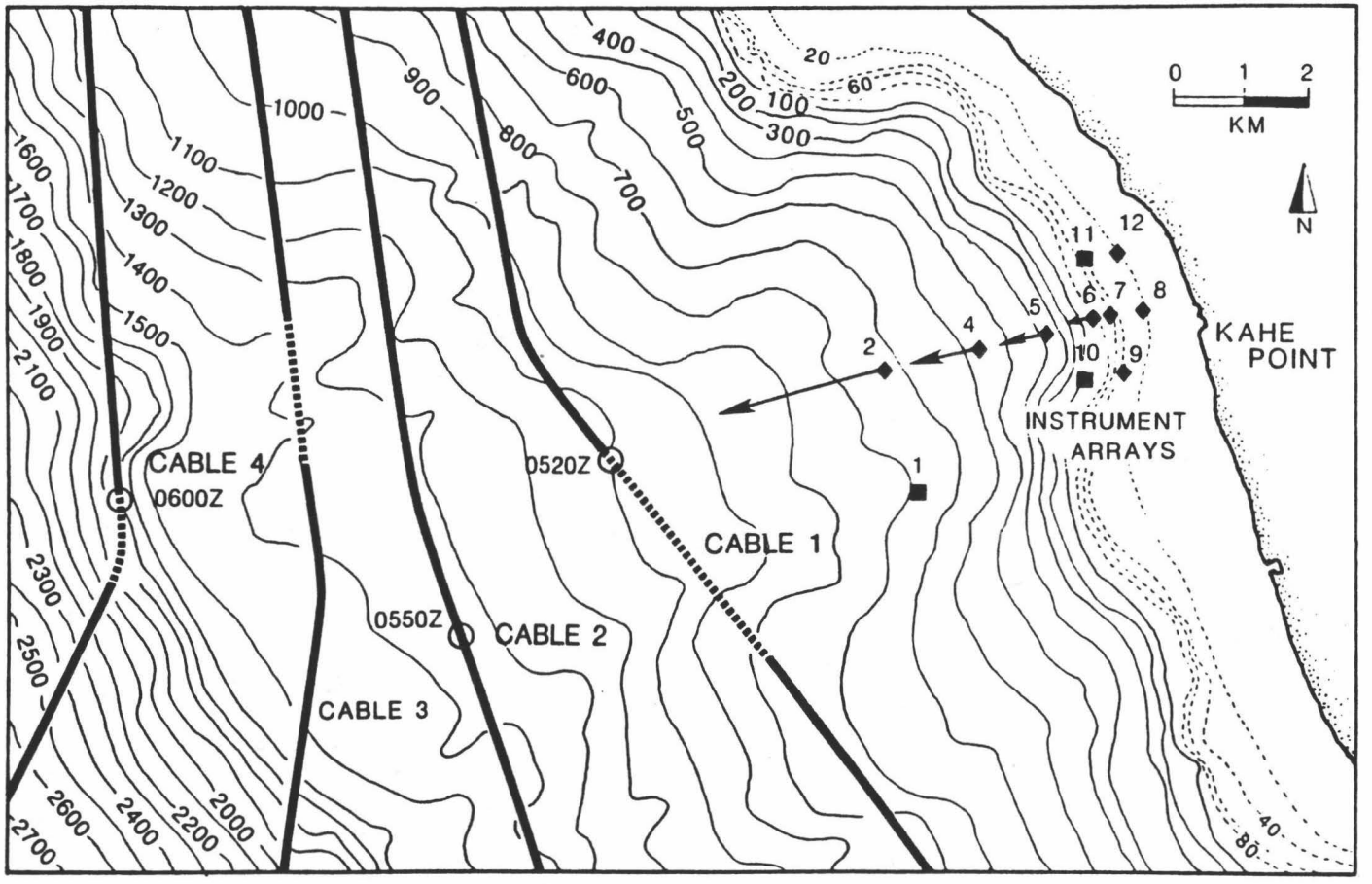

Figure 5. Original positions of instrument arrays and underwater telephone cables off Kahe Point (after Noda, 1983). Squares indicate positions of arrays that were not displaced, diamonds represent positions of arrays that were moved or released during the hurricane and arrows represent estimated movement during the hurricane (Noda, 1983). Circles represent locations of cable breaks and dashed lines mark sections of buried cable. Break times listed are GMT for November 23, 1982.

Damage to the cables occurred in two general areas. Cables 1 to 4 suffered damage to sections located directly offshore the Kahe Point area whereas Cables 5 and 6 were damaged approximately 20 km to the north off Kaena Point (Table 1). The wide separation between sites of damage suggests that sediment movement associated with Hurricane Iwa was not unique to the Kahe Point area.

Instrument Array Movements off Kahe Point

In 1982, the DOE began a study of the thermal regime off Kahe Point using a series of current, temperature and pressure sensor-arrays moored to the ocean bottom (Table 2 and Fig. 5). The arrays which experienced the effects of Hurricane Iwa were set in place on 20 November 1982, and partly recovered on 14 December 1982.

The array moored at position 4 in a water depth of 610 m (2000 ft), apparently surfaced during the passage of Hurricane Iwa on 23 November and was found severely damaged at Barbers Point on 26 November 1982. During recovery operations, the arrays deployed at positions 2, 7, 8, 9 and 12 did not surface nor were they located by divers. Arrays at positions 1, 10 and 11 were found in place. The array at position 6 surfaced seaward of its estimated surfacing point by about 110 to 150 m (350 to 400 feet) and the array at position 5 surfaced approximately 1.2 km seaward of its estimated surfacing point. The array at position 2, considered lost during recovery operations, was subsequently found floating in the Kauai Channel in mid-February, 1983 by a local fishing

Table 2

Location of As-deployed Current Meter Moorings
on November 20, 1982 and Retrieval Information

Current Meter Station No.	As-deployed Location		Water Depth (ft)	Current Meter Locations	Retrieval Information
	Latitude	Longitude			
1	21°20.04′	158°10.47′	2500	33′ off bottom	Retrieved at deployed location
2	21°21.01′	158°10.70′	2500	33′ off bottom	Surfaced Dec. 24, 1982; Recovered mid-Feb. 1983 in Kauai Channel
4	21°21.17′	158°09.96′	2000	33′ off bottom	Surfaced Nov. 23, 1982; Recovered at Barbers Point, Oahu
5	21°21.34′	158°09.31′	1300	33′ off bottom	Retrieved at 21°21.21′/158°09.96′ about 1.2 km seaward of deployed location
6	21°21.45′	158°08.86′	345	33′ off bottom, 180′ fm surface	Retrieved 125 m seaward of deployed location
7	21°21.46′	158°08.81′	260	33′ off bottom, 135′ fm surface	Not recovered
8	21°21.49′	158°08.48′	80	15′ off bottom	Not recovered
9	21°21.01′	158°08.61′	80	15′ off bottom	Recovered May 1983 at Kahe Point
10	21°21.91′	158°08.97′	263	33′ off bottom, 138′ fm surface	Retrieved at deployed location

/continued...

Table 2. (continued) Locations of As-deployed Current Meter Moorings on November 20, 1982 and Retrieval Information

Current Meter Station No.	As-deployed Location		Water Depth (ft)	Current Meter Locations	Retrieval Information
	Latitude	Longitude			
11	21°21.88′	158°09.12′	250	33′ off bottom, 125′ fm surface	Retrieved at deployed location
12	21°21.93′	158°08.72′	95	15′ off bottom	Recovered Dec. 1983 at Maili Point

(after Noda, 1983)

vessel. Array 9 washed ashore during March and array 12 during September, 1983; arrays 7 and 8 have not yet been recovered.

Recordings of current velocity for all recovered sensors show fluctuations during passage of the storm. Recordings of water pressure and current velocities on arrays 2, 4, 5 and 6 exhibited rapid increases commencing with the closest approach of the hurricane (Noda, 1983). Estimates of downslope movement for these arrays are based on the recorded changes in pressure (Noda, 1983). Most of the storm-related movement was concentrated in a narrow path perpendicular to shore and involved arrays 2, 4, 5, 6, 7, and 8 (Fig. 5).

HECO environmental monitoring teams found a loss of sand from shallow areas off Kahe Point during Hurricane Iwa. Sixteen measuring rods were sunk into the sand between shore and 20 m (66 ft) depth and after the passage of the hurricane only two remained (circles on Fig. 3). Both rods indicated decreases in sand thickness of more than 1.5 m (Coles, 1984). No quantitative estimate of total sand loss from the area was made but observations by the HECO divers indicate that most of the reef surface was swept clean of sediment cover and that most of the damage to the reef itself occurred at 6 m (20 ft) depth or below (Peck and Fukuda, 1985, pers. comm.).

Causes of Movements and Damages

Noda (1983) suggested turbidity flows as one of the possible causes of the cable breaks and instrument movements. Dengler et al. (1984) expanded on this idea, attributing the cable breaks and array

movements to turbidity currents triggered by slope failures. Fornari (1984) suggested that the array movements were caused by breaking internal waves and largely discounted turbidity flows or mass movement, stating that "the nature of the escarpment suggests that the escarpment did not fail and has not been subjected to mass wasting since the last lowering of sea-level." Hollister (1984) stated that several smaller debris flows, triggered by shoaling or breaking internal waves, were responsible for the array movements, and that the cables were broken by chafing against rough bottom.

FIELD WORK

Cruises and Navigation

Most of the data utilized in this study were collected during 1983-84 cruises of the University of Hawaii research vessel R/V Kana Keoki, in the course of a series of dives by the U.S. Navy submersible DSV Turtle, and during a February, 1985 cruise of the U.S. Navy research platform SSP Kaimalino. Information collected on these cruises includes detailed SeaMARC II side-scan sonar imagery and high-resolution bathymetry, 3.5 kHz seismic reflection profiles, ocean bottom photographs and both piston and box cores.

Precision navigation on all but one of the Kana Keoki cruises was obtained with a Del Norte Trisponder micro-wave transponder system. Recorded distances are theoretically accurate to within +/- 3 m over an operating range of 85 km, but the absolute accuracy is probably closer to +/- 10 m. This high precision allows accurate location of sample stations on the detailed structures revealed on the SeaMARC II images.

Shore-transponder beacon stations were located at the U.S. Coast Guard lighthouse at Barbers Point, the Hawaiian Electric Company Stack #2 located at Kahe Point and the U.S. Navy North FORACS range tower located at Maili Point (Fig. 1).

SeaMARC II Survey and Images

SeaMARC II is a long range, side-scan sonar, remote sensing and mapping system capable of producing images and high resolution bathymetry of the ocean bottom. The system uses two rows of 11 and 12 kHz side-looking sonar transmitter/receivers, each of which sends out signals in parallel, but measures returning echoes separately. The acoustic travel time and the angle of echo arrival determine depth and distance of the object or surface reflecting the signal. Side-scan images are a combination of micro- and macro-reflectors (Blackinton et al., 1983). Micro-reflectors are a result of bottom detail which possesses dimensions of less than 12 cm, which approximately equals one wavelength of the energy utilized by the SeaMARC II system. Macro-reflectors consist of specular (flat surface) images resultant from objects or surfaces greater than 12 cm (Blackinton, 1985, pers. comm.). The result, an acoustic image of the ocean bottom, is similar in aspect to aerial photography. The system also produces a bathymetric contour chart with a resolution of 1% of the water depth. Technical specifications and details of the system of operation are presented by Blackinton et al. (1983).

A first set of side-scan sonar data was collected during a test-cruise for the SeaMARC II system in September of 1983. Positions during this survey were obtained by dead-reckoning and standard radar navigation and may be in error by as much as 0.5 km (Campbell, 1984, pers. comm.). The images produced were used as a preliminary guide for subsequent bottom sampling, bottom photography and more detailed

SeaMARC II surveys for cruises during March (Fig. 6) and April, 1984 and February, 1985. The final SeaMARC II side-scan sonar mosaic is displayed in Figure 7.

Core Collection

A total of 17 piston cores and 2 box cores was collected from the study area during two R/V Kana Keoki cruises in March and April, 1984 (Fig. 8). This study concentrates on piston cores PC-15, PC-16, PC-17, PC-18 and PC-19, sampled and analysed at HIG. Grain-size distributions for samples from the remaining cores were provided by the Earth Technologies Corporation (ERTEC). Unfortunately, these cores were not available for direct sampling and analysis.

Ocean Bottom Photography

The seafloor was photographed directly from the U.S. Navy submersible DSV Turtle during a series of dives in 1983 (Fornari, 1983) and with a bottom camera towed from the U.S. Navy research platform SSP Kaimalino in February, 1985 (Fig. 9). Positions for the Turtle surface support-vessel were plotted using a Mini-Ranger electronic navigation system similar in accuracy and operation to the Del Norte Trisponder system used during the R/V Kana Keoki and SSP Kaimalino cruises. Submersible positions were determined using an acoustic navigation system in contact with the support-vessel.

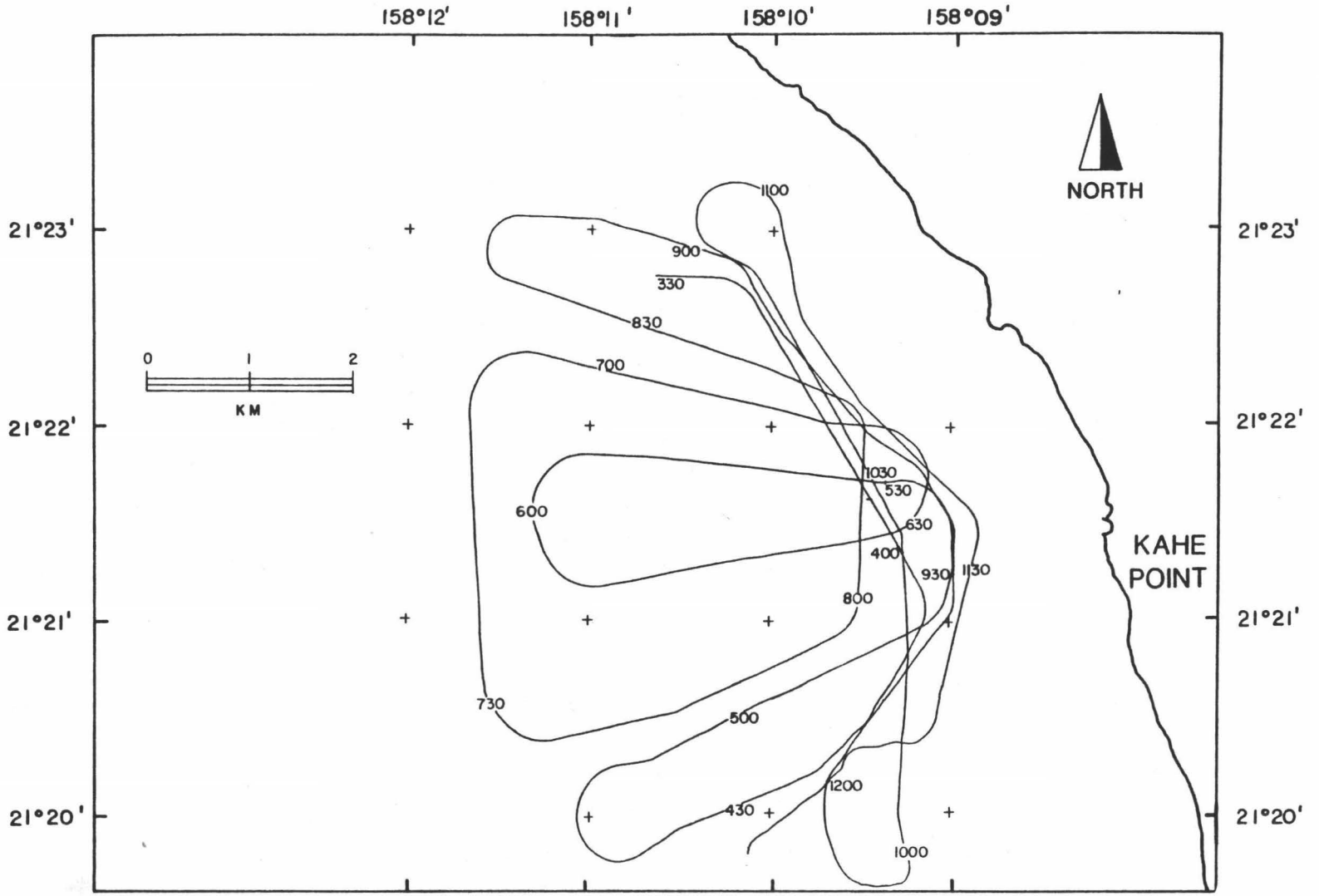

Figure 6. Trackplot of SeaMARC II survey KK84-03-06. Times listed are GMT for March 7, 1984.

Figure 7. Detailed mosaic of SeaMARC II side-scan sonar images of the Study area off the southwest Waianae coast. Trackplot shown on Figure 6.

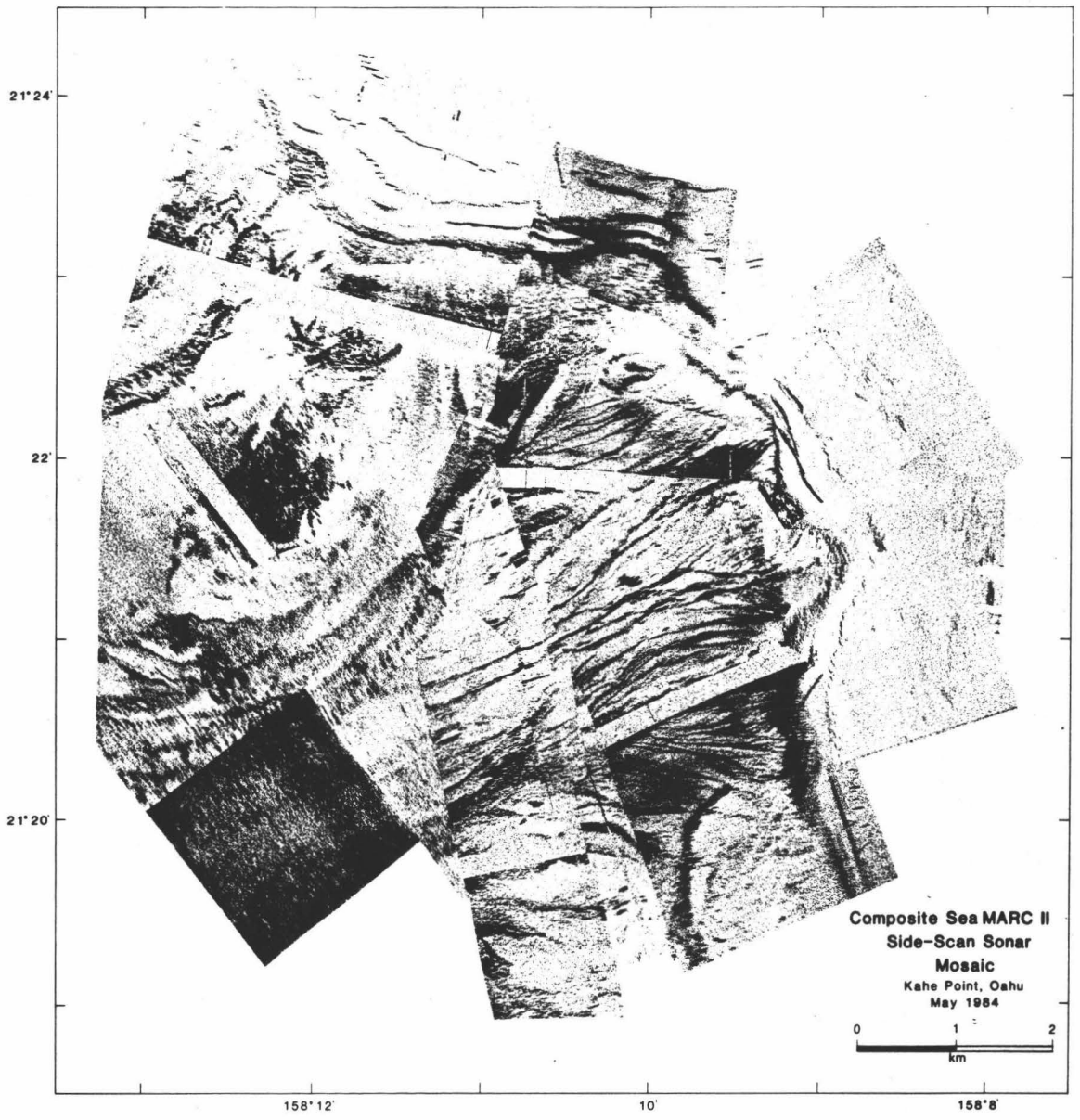
21°24'
22'
21°20'
158°12'
10'
158°8'
Composite Sea MARC II
Side-Scan Sonar
Mosaic
Kahe Point, Oahu
May 1984
0
1
2
km

Figure 8. Piston core (triangles) and box core (squares) sampling stations for R/V Kana Keoki cruises KK84-03-06 and KK84-04-06 superimposed on an interpretation of the SeaMARC II mosaic shown in Figure 7. Solid lines indicate sharp reflection boundaries shown in SeaMARC II images and dot-dash lines indicate gradational reflection boundaries. Patterns for shelf cover based on Campbell et al. (1970).

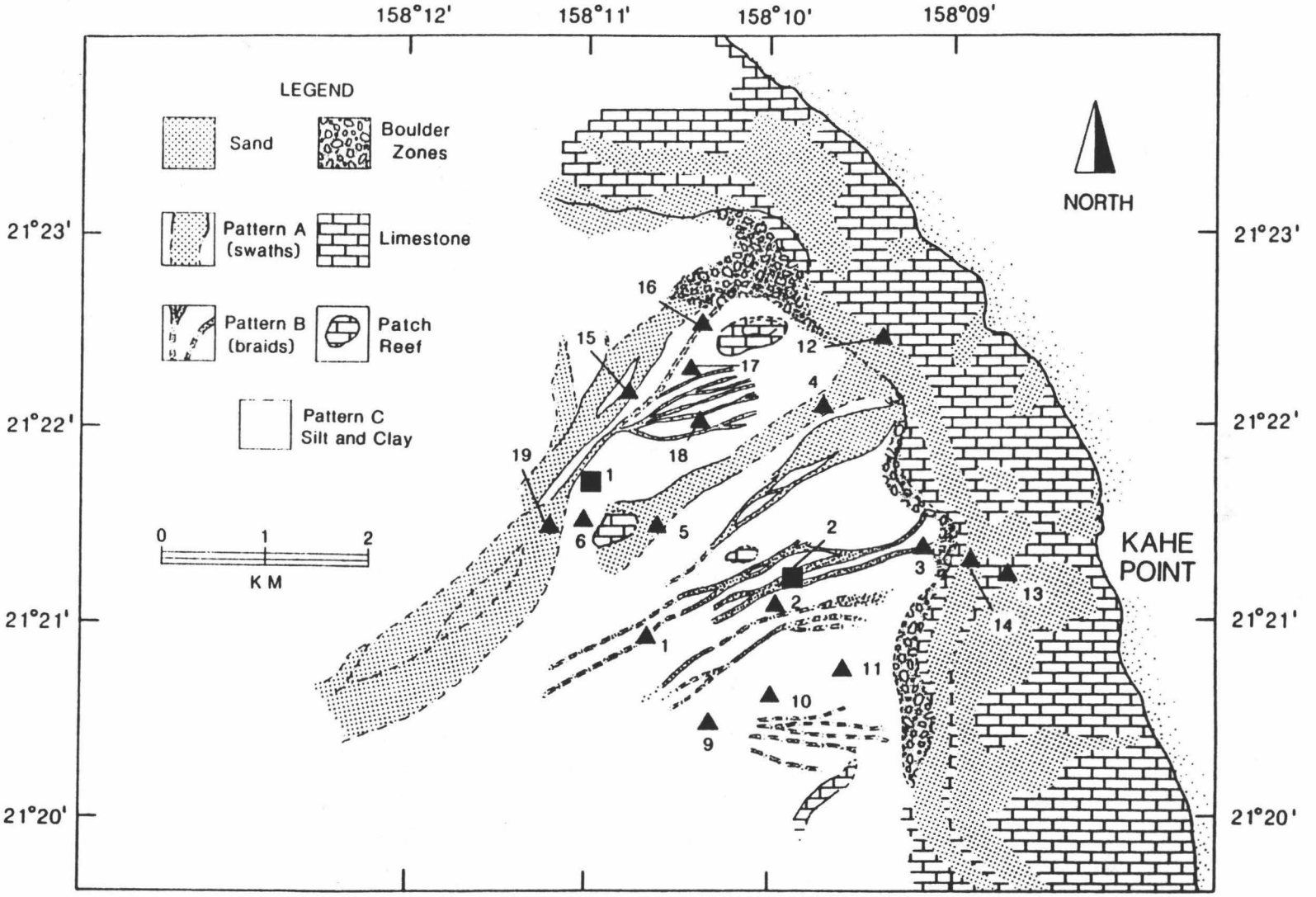
158°12'
158°11'
158°10'
158°09'
21°23'
21°22'
21°21'
21°20'
LEGEND
Sand
Boulder Zones
Pattern A (swaths)
Limestone
Pattern B (braids)
Patch Reef
Pattern C Silt and Clay
0 1 2
K M
NORTH
KAHE POINT
1
2
3
4
5
6
9
10
11
12
13
14
15
16
17
18
19

Figure 9. Submersible dive tracks (dot-dash lines) for DSV Turtle, 1983 and bottom camera tows (solid lines) by the SSP Kaimalino, 1985. Submersible tracks after Fornari (1983). Circles locate positions of example bottom photographs.

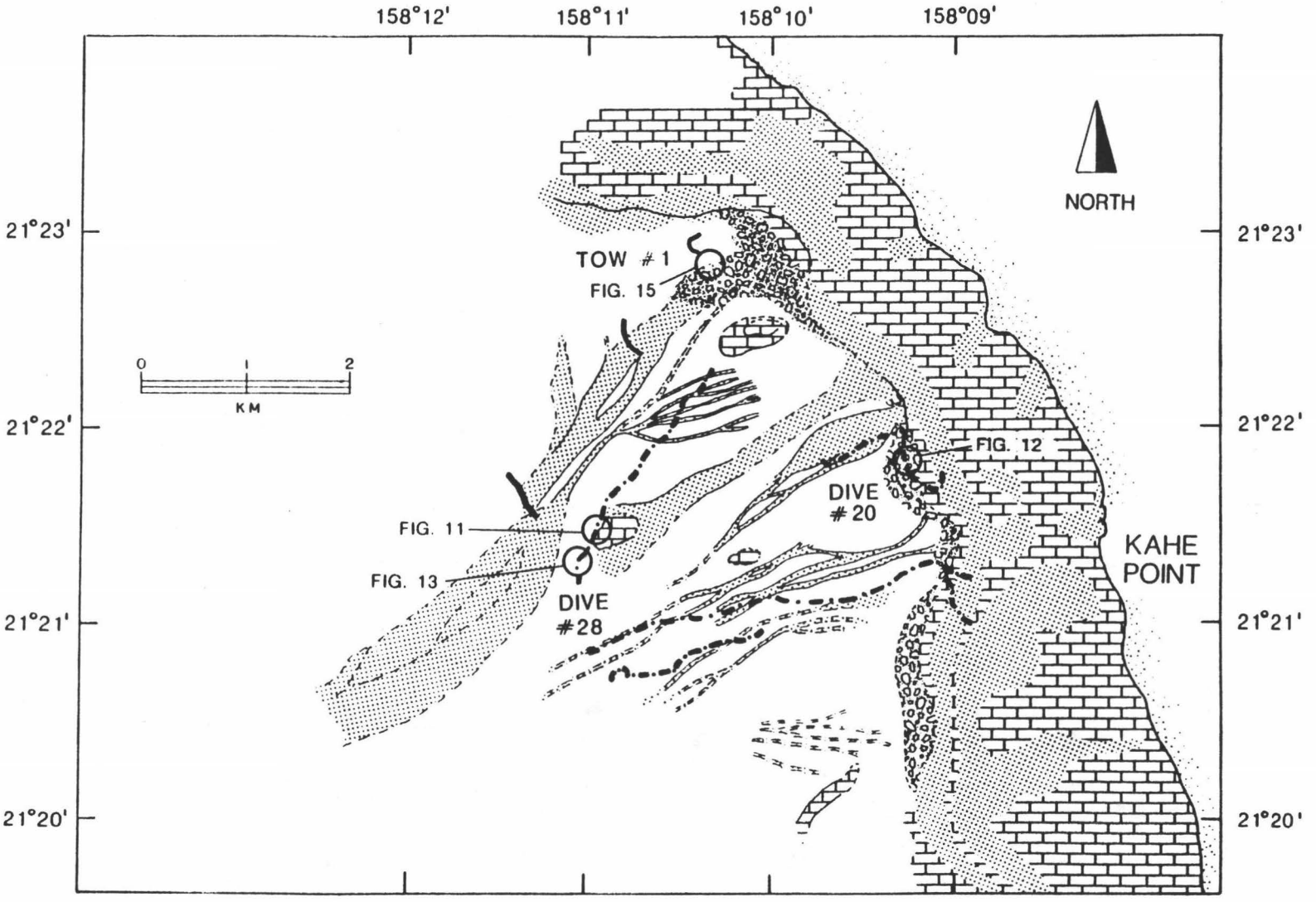
158°12'
158°11'
158°10'
158°09'
21°23'
21°22'
21°21'
21°20'
NORTH
TOW # 1
FIG. 15
0
1
2
KM
FIG. 12
DIVE
20
FIG. 11
FIG. 13
DIVE
#28
KAHE
POINT

LABORATORY SAMPLING AND ANALYSIS

Sample Size and Preparation

Core samples of approximately 3 cc were collected routinely at intervals of 50 cm and the cores were resampled at closer intervals on the basis of lithologic changes. Each sample was disaggregated with a 2% Calgon solution and washed three times with a solution of acetone and distilled water to remove soluble salts contained in the pore water.

Grain-size Determination

Samples were wet sieved through a 4.0 phi (.063 mm) mesh sieve with distilled water to separate silt and clays from the sand and gravel. The wash water containing the fine fraction was retained. The grain-sizes larger than 4.0 phi were dried and sieved through meshes ranging from -2.0 phi (4 mm) to 4.0 phi (.063 mm) at 0.5 phi increments. Any remaining residue was added to the wash water containing the fine fraction. Weight percents of the silt and clay fractions were determined using standard settling-tube and pipette procedures (Lewis, 1985). Consistency and reproducibility of both the sieve and the settling tube procedures were tested by analysing five 3 cc replicate samples collected from PC-17. The resulting distributions were tested for equality of the means between replicates using an analysis of variance (ANOVA) program (modified after Davis, 1973).

Grain sizes for samples from the ERTEC cores were determined using ASTM mesh sieves and by hydrometer (Brylawski, 1984). Because the ASTM standards are not based on the Wentworth phi scale used in this study, ERTEC data were converted to equivalent phi increments by interpolating points off plots of the size distribution curves.

A FORTRAN routine was used to compute values for mode, mean grain size, standard deviation (sorting) and skewness for each sample distribution (Table 3) according to the method of moments (see Griffiths, Table 5.4, 1967). Grain-size distributions of core-top samples are grouped by computing a matrix of correlation coefficients and clustering these according to the weighted pair-group analysis (WPGA) method outlined in Davis (1973). Groupings were tested for distinctiveness by applying a discriminant analysis (Jennrich and Sampson, 1979).

Micropaleontological Sampling and Analysis

Samples of one to two grams were taken for micropaleontological analysis at the same intervals as those taken for grain size. Samples were disaggregated, dried and reduced by microsplitter to splits of about 0.3 to 0.5 gm. At least 300 individual foraminifera were counted for each sample, using more than one split where necessary. Individuals were identified to the species level and, where possible, were classified according to their normal depth of occurrence. A total of 68 species was identified. Species were grouped into shallow benthic (SB) species normally dwelling on the shelf at depths less than

Table 3

Grain-size Parameters for Kahe Point Core-top Samples*

Core Location Numbers	Mode**	Mean**	Standard Deviation**	Skewness
PC-01-000	2.25	2.26	0.41	0.41
PC-02-000	5.25	4.85	0.43	-0.48
PC-03-000	0.25	0.42	0.64	0.23
PC-06-000	7.25	6.24	0.73	0.06
PC-09-000	6.25	5.42	0.62	0.07
PC-10-000	7.25	6.17	0.79	0.04
PC-12-000	3.75	2.99	0.77	-0.28
PC-13-000	3.25	3.01	0.65	-0.65
BC-01-000	7.25	6.17	0.77	-0.02
BC-02-000	2.25	2.17	0.63	-0.17
PC-15-000	3.75	3.76	0.33	-0.19
PC-16-000	3.75	3.60	0.38	-0.44
PC-17-000	5.25	5.03	0.57	0.09
PC-18-000	5.25	5.10	0.60	0.11
PC-19-000	3.24	3.27	0.36	0.48

** Phi Units

100 to 120 m (330 to 360 ft), deep benthic (DB) species dwelling at depths below the 100 to 120 m shelf-break and planktonic (P) specimens. Benthic species whose depth zonations were too broad or unknown were set aside (Table 4).

Table 4

Foraminiferal Species Found in Core Samples off the Southwest Waianae Coast

PLANKTONIC SPECIES:

Globorotalia menardii	Globigerinoides ruber
tumida	sacculifer
crassula	quadrilobatus
crassaformis	immaturus
Globigerinella aequilateralis	
calida	Globigerina rubescens
obesa	quinqueloba
Orbulina universa	Turborotalia cristata

SHALLOW BENTHIC SPECIES:
(most common occurrence above 100-120 m water depth)

Amphistegina lobifera	Quinqueloculina granulocostata
lessonii	parkeri
	bosciana
Peneroplis planatus	distorqueata
	lamarckiana
	laevigata
Amphisorus hemprichii	poeyana
Cymbaloporetta bradyi	Spiroloculina corrugata
	communis
Fijiella simplex	
Hauerina pacifica	Triloculina oblonga
	trigonula
Gaudryina siphonifera	
	Elphidium articulatum
Rosalina floridana	poeyana
Florilus japonicus	Spirillina inaequalis
Articulina carinata	Pyrgo denticulata
Bolivina striatula	Miliolinella subrotunda
Sorites marginalis	

/continued...

Table 4. (Continued) Foraminiferal Species Found in Core Samples From off the Southwest Waianae Coast

DEEP BENTHIC SPECIES:
(most common occurrences below 100-120 m water depth)

Amphistegina bicirculata

Cymbaloporetta squammosa

Uvigerina asperula

Cibicidoides pseudoungerianus

Hoeglundina flinti

Textularia agglutinans

Cassidella schreibersiana

Bueningia creeki

Eponides repandus

Trifarina bradyi

Bolivina glutinata
pacifica
compacta
rhomboidalis

Cassidulina sulcata
radiata
crassa (auct)
patula
oriangulata

UNKNOWN:
(broad depth range or not available)

Cibicides lobatus

Fissurina sp.

Rosalina concinna

Globobulimina sp.

References:

Chave (1985, in press)
Cushman, Todd and Post (1954)
Kennett and Srinivasan (1980)
Loeblich and Tappan (1964)
Murray (1973)
Phleger (1960)
Resig (1969)

SeaMARC II PATTERN RECOGNITION

The SeaMARC II side-scan sonar images were compared with corresponding bathymetry and 3.5 kHz seismic reflection profiles. Ground truth was provided by comparing the geophysical interpretations with features seen on bottom photographs and in surface sediments. Darkness of tone on the SeaMARC II images increases with degree of reflectivity of the ocean bottom. These gray tones are caused by distinct changes in bottom slope, varying surface texture or sediment roughness. For example, steep slopes are generally highly reflective and produce darker tones.

The final SeaMARC II mosaic (Fig. 7) reveals features not detected by earlier, more conventional survey efforts. The sea floor is complex and varied, generating four main types of reflections:

(1) reflectors from escarpments

A band of distinct and continuous reflectors that are imaged as uniform dark gray to black patterns trends roughly parallel to the coast and delineates the steep face of the escarpment above the Lualualei shoreline (Figs. 7 and 10). This feature corresponds to the steep slope between the 90 to 360 m (300 to 1200 ft.) depth contours on the SeaMARC II bathymetry. Shadow effects from sections of this steep slope can locally obscure other reflective patterns.

Figure 10. High resolution SeaMARC II bathymetry, Kahe Point study area. Contour interval 30 feet. Dashed lines indicate areas of sparse coverage and question marks indicate areas of no coverage.

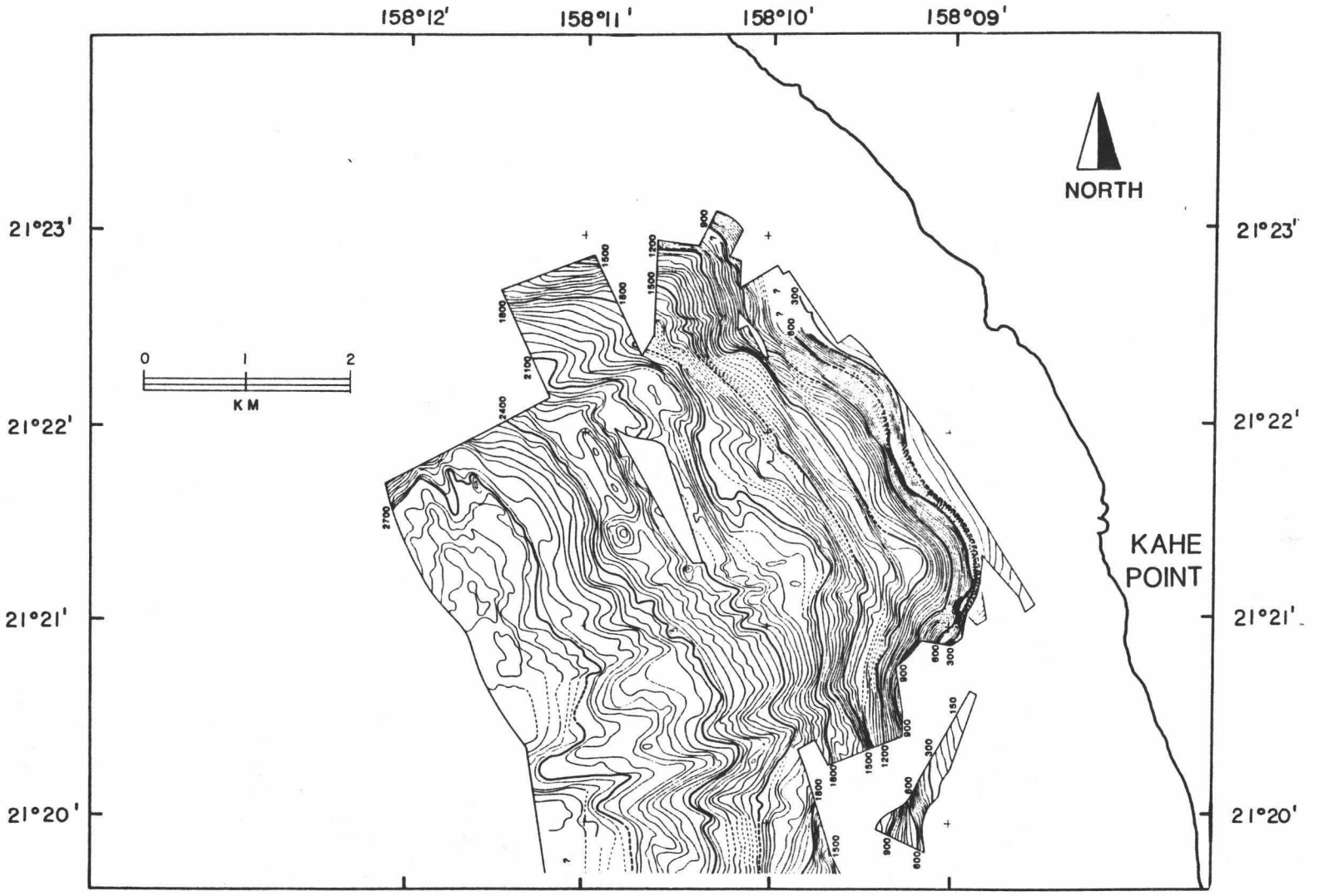
158°12'
158°11'
158°10'
158°09'
21°23'
21°22'
21°21'
21°20'
NORTH
KAHE
POINT
0
1
2
KM

(2) reflectors from isolated, positive relief features--

Four isolated, sharply-defined, crescentic patterns of gray to black reflectors correspond to features of positive relief clearly visible on the SeaMARC II bathymetry (Figs. 7 and 10). One of these is located in the middle of the re-entrant and corresponds to a distinct, dome-like feature lying between 650 and 715 m (2100 and 2400 ft). Bottom photographs reveal a drowned patch reef at this position (Fig. 11). The other three features of this type also probably represent drowned patch reefs.

(3) reflectors from boulder zones

The mosaic displays a narrow and uneven ribbon of predominantly dark gray tones paralleling segments of the escarpment base. These tones are interspersed with uneven, light gray and black tones which form tiny acoustic shadows (Fig. 7). Ocean bottom photographs show boulders, rock debris and coarse sediment in these areas (Figs. 9 and 12). The boulders range in size from 0.5 to 3.0 m (Fornari, 1983).

(4) reflectors from finer sediment cover--Patterns A, B and C

This group comprises three different types of gray tones which represent zones located seaward of the base of the escarpment. The first group (Pattern A) consists of large, broad swaths of uneven light gray to black tones. This pattern represents sediment cored at PC-15,

Figure 11. Bottom photograph of drowned patch reef--DSV Turtle dive 28. Location of photograph shown of Figure 9. Reef outcrops diagonally, separating fine sand and silt cover on upper left corner from silt mantled slope below reef edge in lower right corner.

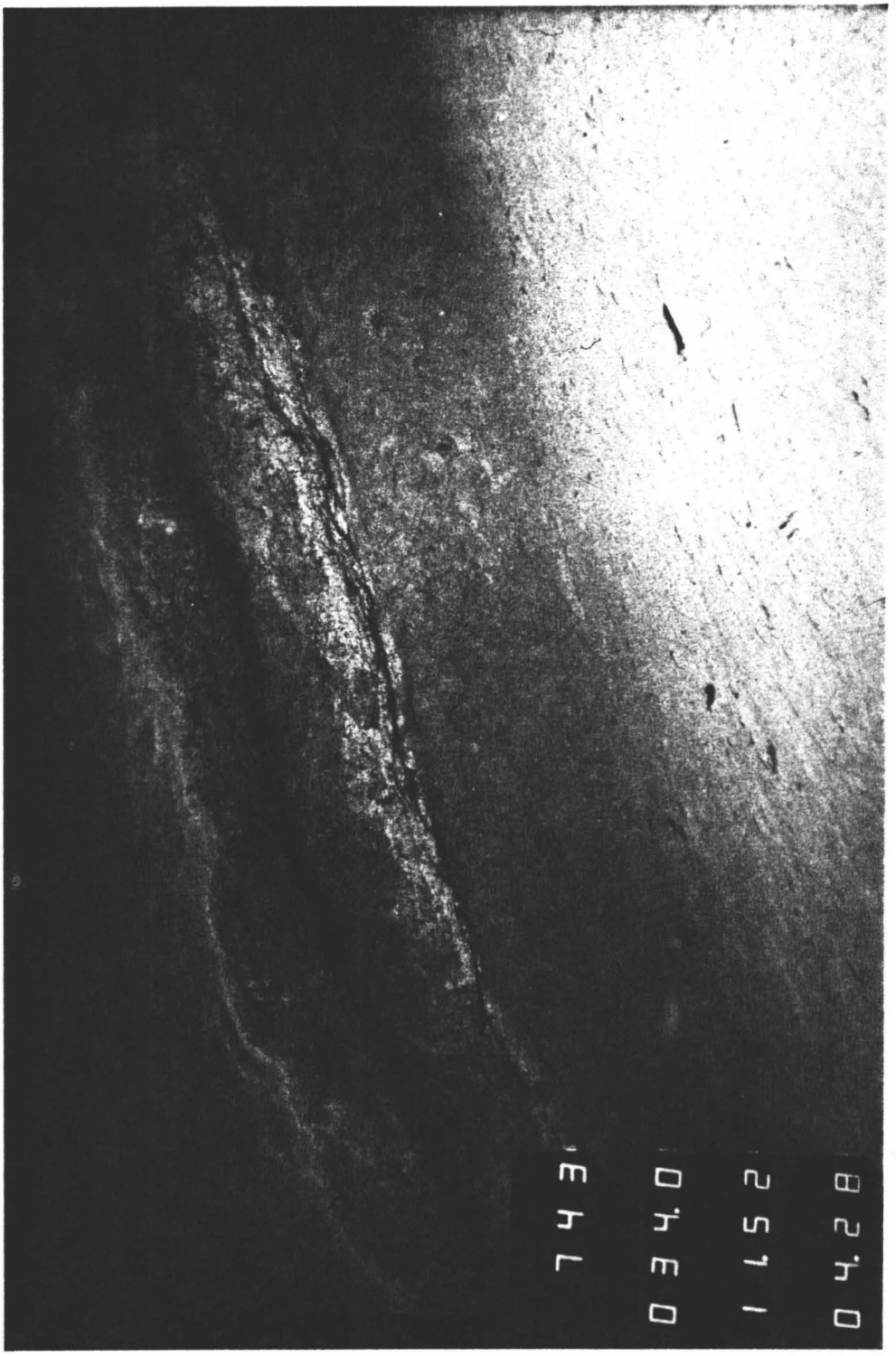
0h28
2511
0h30
74E

Figure 12. Bottom photograph of boulder zone--DSV turtle dive 20. Location of photograph shown on Figure 9.

PC-16 and PC-19 (Fig. 8). Light gray tones (Pattern B) identify sharply defined features cored at PC-1, PC-3 and BC-2. The third group is the background of even, white to light gray tones covering most of the mosaic (Fig. 7). Cores PC-17 and PC-18 were collected from areas exhibiting Pattern C.

PATTERNS AND ASSOCIATED SEDIMENT

Pattern C--Background Cover

Areas showing uniform, very light gray to white tones are designated as Pattern C, representing most of the area seaward of the base of the re-entrant. Bottom photographs consistently show that Pattern C is smooth sediment cover (Fig. 13).

Pattern C Cores--PC-17 and -18

Cores PC-17 and -18 were collected from areas represented as Pattern C (Fig. 8). The cores are composed of thick sequences of silt and clay interrupted by distinct coarse layers of sand and gravel (Fig. 14). The silt- and clay-sized fractions are predominantly calcite, made up of small deep benthic (DB) and planktonic (P) foraminifera and fine reef detritus. Coloring of these sediments ranges from 5Y 6/2, light olive gray, to 2.5Y 7/2, light brownish gray according to the Munsell color scale. These fine-grained sediments contain only trace amounts of clay minerals. X-Ray diffraction (XRD) patterns show questionable peaks indicating the presence of halloysite.

Lithology, grain-size and foraminiferal percentages change within the coarse layers (Fig. 14). For example, the sub-bottom sequence from 380 to 250 cm in PC-18 initially displays fine silt and clay interrupted by a sharp boundary at 375 cm. Concurrent rapid increases in grain-size, in relative percentage of shallow benthic (SB)

Figure 13. Bottom photograph showing smooth sediment cover forming light background areas (Pattern C) of SeaMARC II mosaic (Figure 7)--DSV Turtle dive 28. Location of photograph shown on Figure 9.

7 5 1
3 5 8.0
1 1 4 6
2 2 8

foraminifera and in clay minerals halloysite and smectite occur immediately above this boundary. Colors exhibited by these layers range from 2.5Y 3/2, very dark grayish brown, to 5Y 3/2, dark olive gray on the Munsell color scale. Irregular changes of SB foraminiferal percentages and inverse size grading are present above the boundary. From about 300 cm sub-bottom depth, grain-size gradually fines upwards, and percentages of SB foraminifera gradually decrease (Fig. 14).

Pattern A--Swaths of Rough Sediment

The clearest and largest example of Pattern A is in the northern corner of the re-entrant directly seaward of the locations of the thickest shelf-edge sand wedges mapped by Campbell et al. (1970). The reflections from these areas form swaths of uneven tones of gray to black which include occasional speckles of light gray. These swaths stream downslope from the base of steeper sections of the re-entrant, trend roughly perpendicular to the depth contours, overlap each other and interrupt background areas displaying Pattern C (Fig. 7). Reflective patterns of this type are interpreted as representing small-scale (<12 cm) roughness of the seafloor or coarse sediment cover (Campbell, 1985, pers. comm.). Photographs of this ocean bottom (Fig. 15) reveal that the surficial sediment is coarser than the sediment cover from Pattern C areas. The differences in appearance (compare Figs. 13 and 15) are minor, however, compared to the differences in reflectivity registered on their respective SeaMARC II images (Fig. 7). Acoustic energy from the 11 and 12 kHz transducers may penetrate as

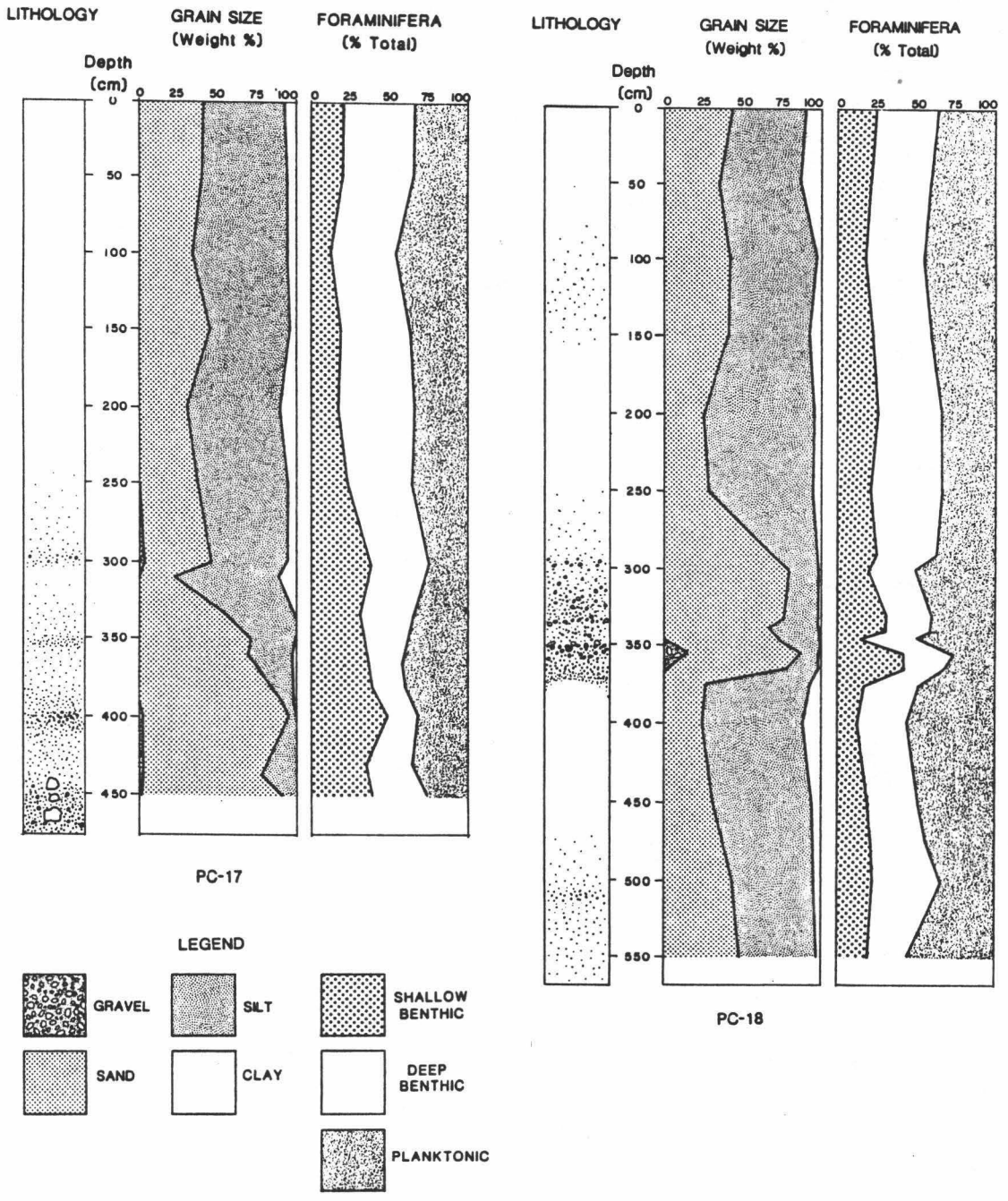

Figure 14. Lithology, grain size and foraminiferal percentages for PC-17 and PC-18 collected from areas represented by Pattern C in the northern part of the study area.

Figure 15. Bottom photograph showing a Pattern A surface--SSP Kaimalino camera tow 1. Location of photograph shown on Figure 9.

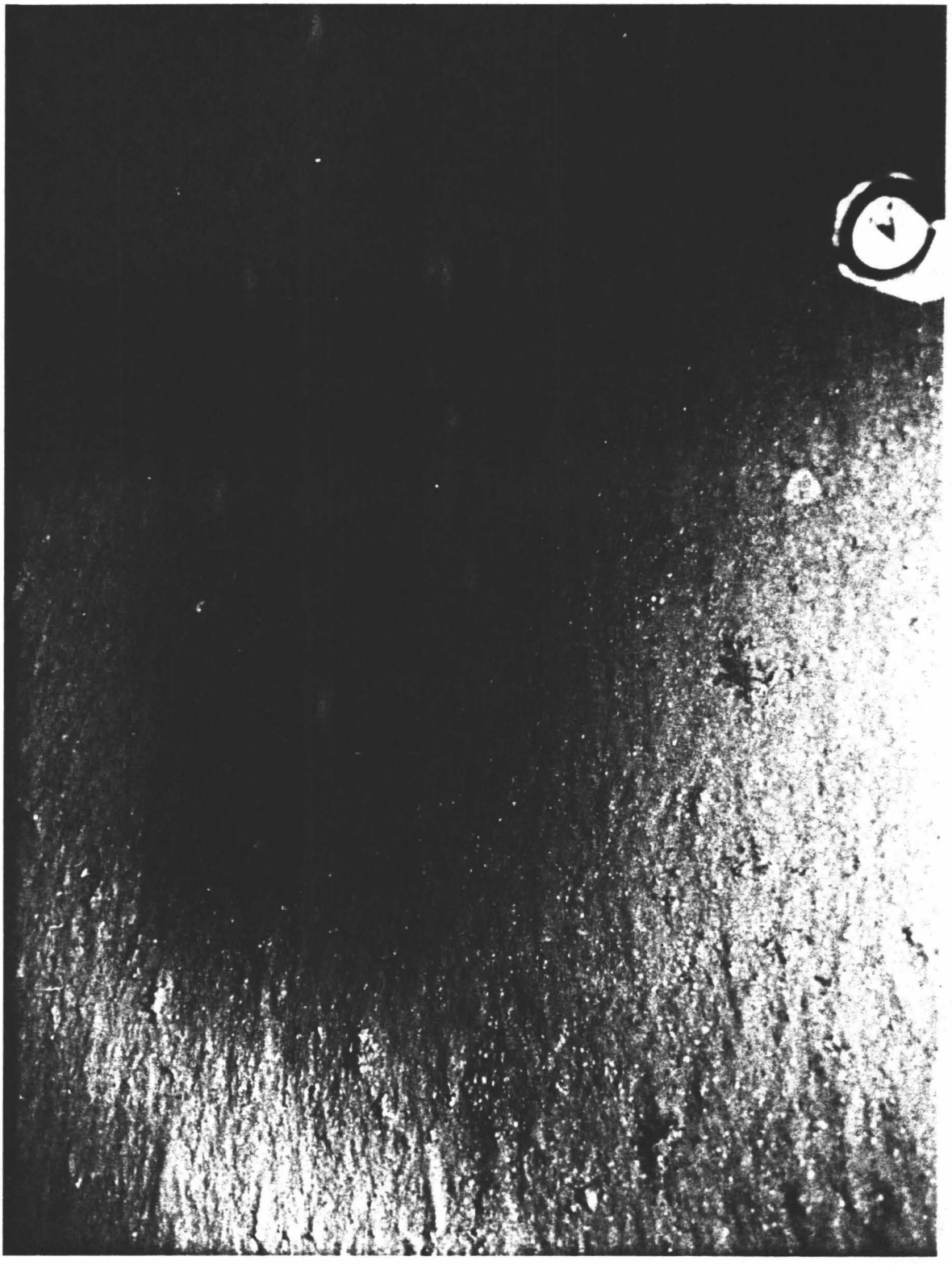

much as a meter of sediment, especially if that sediment is fine-grained (Campbell, 1985, pers. comm.). SeaMARC II images may therefore, in some instances, measure the attributes of the very shallow subsurface material and treat the surficial fine-grained cover as acoustically transparent. Farther upslope, a thin veneer of fine sediment covers rock surfaces along the lower escarpment face and boulder zone (Fornari, 1983). If a veneer has had time to accumulate in this relatively steep and very rough substrate, such a thin veneer may also hide coarseness of sediment in Pattern A swaths.

Pattern A Cores--PC-15, -16 and -19

Cores PC-15, -16 and -19 were collected from within the largest example of Pattern A (Figs. 7 and 8). The cores contain very poorly sorted, angular, coarse-sands and gravels ranging from 10YR 6/2, light brownish gray, to 2.5 Y 6/2 on the Munsell color scale (Fig. 16). Grain size, relative percentages of shallow benthic (SB) deep benthic (DB) and planktonic (P) populations and, in the case of PC-19, occurrence of clay minerals, reveal only minor fluctuations throughout the cored intervals (Fig. 16). These cores contain uniformly high percentages of SB foraminifera, in particular the species Amphistegina lobifera and A. lessonii. These large, very robust species normally dwell on shallow reef flats (Chave, 1985, in press), and make up a large proportion of beach sands around the Hawaiian Islands. The specimens of these species in Pattern A cores are very distinctive and

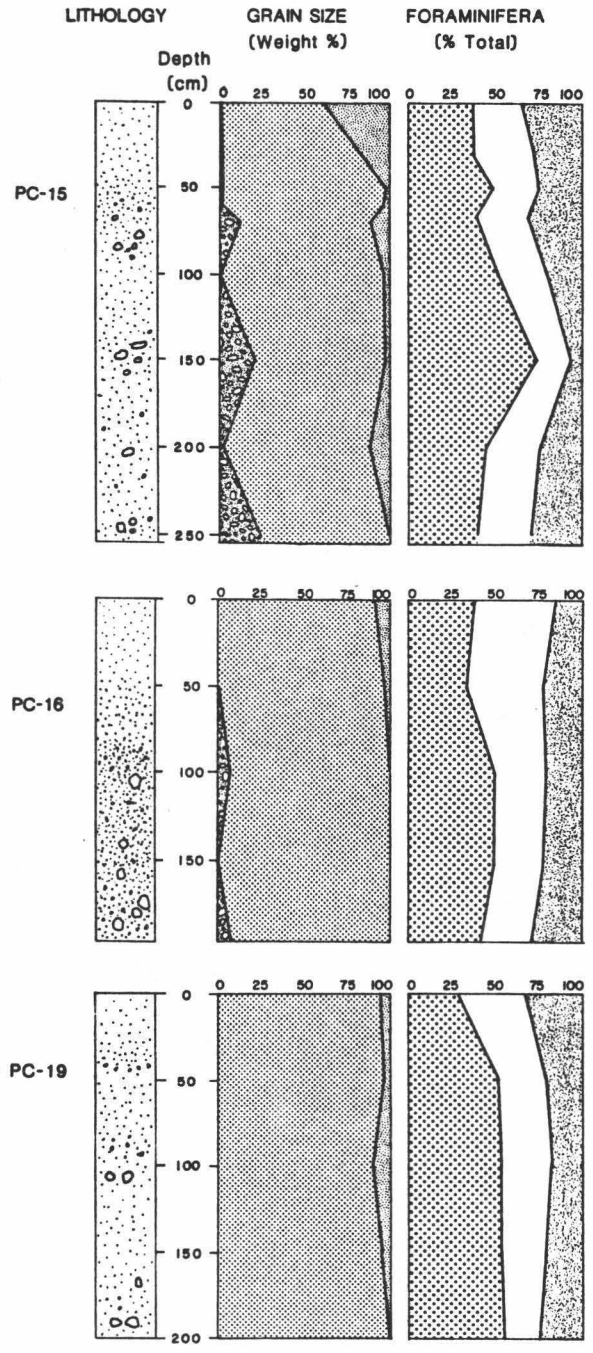

Figure 16. Lithology of grain-size and foraminiferal percentages for cores collected from areas represented by Pattern A on the SeaMARC II images (Figs. 7 and 8). For lithological legend refer to Figure 14.

easily identified, and show a wide range of abrasion and wear. The gravel fraction is comprised predominantly of coral fragments.

Pattern B--Braids of Rough Sediment

The largest and most distinct examples of Pattern B are located in the southern corner of the re-entrant. Their landward terminus at the base of the escarpment lies directly downslope of thick sand wedges mapped at the shelf-edge (Fig. 8).

These pattern B areas are long, sinuous, narrow and sharply defined, often showing positive relief (Fig. 7). The patterns are uniformly gray, slightly darker than the light gray to white Pattern C tones that they interrupt. They generally trend perpendicular to the depth contours and are located below moderately sloping sections of the escarpment. Inflections in depth contours characterize Pattern B areas (Fig. 10). Superposition of the pre-hurricane instrument array positions on the interpretation of the SeaMARC II mosaic reveals that displaced arrays 2, 4, 5 and 6 were originally located upon sea-floor presently showing Pattern B (Fig. 17). In addition, the estimated direction of array movement downslope during the hurricane roughly matches with the downslope trend of these patterns.

Pattern B Cores

ERTEC cores PC-1, BC-2 and PC-3 were collected from within the largest example of Pattern B (Fig. 8). Data on grain-size

Figure 17. Hurricane Iwa related instrument array movements and underwater cable damage superimposed upon an interpretation of the SeaMARC II mosaic. Lithology and symbols are the same as those used in Figures 8 and 5, respectively.

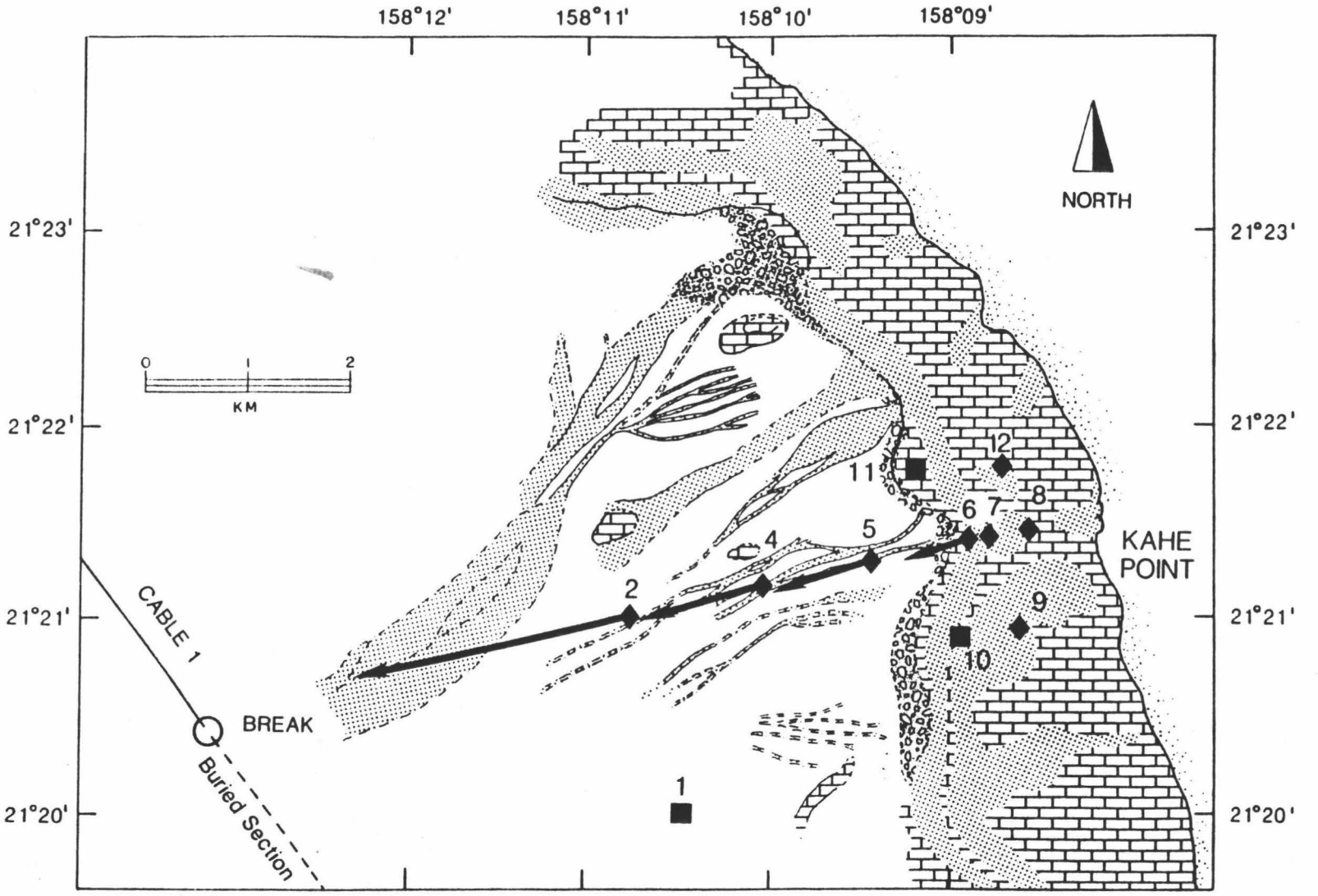
158°12'
158°11'
158°10'
158°09'
21°23'
21°22'
21°21'
21°20'
NORTH
0
1
2
KM
CABLE 1
BREAK
Buried Section
KAHE
POINT
1
2
3
4
5
6
7
8
9
10
11
12

distributions and simplified core logs were provided by ERTEC, but no actual samples were made available for analysis. The grain-size distributions of sediments within the cores indicate medium sand in PC-1 and BC-2, and gravel in PC-3 (Fig. 8).

Statistical Analysis of Core-top Grain-size Distributions

A cluster analysis reveals the similarity of grain-size distributions for 15 core-top samples (Table 3, Fig. 18a). The structure of the dendrogram can be interpreted in terms of three groups and two outliers. Samples forming Group 1 were all collected from smooth, low-reflectivity areas represented by Pattern C. The grand mean of grain-sizes for these samples is 5.7 phi, medium to fine silt, which is moderately well sorted (sigma = 0.68 phi) and displays a symmetric distribution (SK = 0.06). Samples forming Group 2 were collected from within the largest example of Pattern B. These samples have a grand mean grain-size of 2.21 phi, medium sand, with sigma = 0.52 phi. A skewness of 0.29 indicates that these distributions possess an excess of fine material (Folk, 1975). The Group 3 samples include cores collected from Pattern A, along with the two cores, PC-12 and PC-13, which were collected from the sand wedges located on the Mamala-Kahipa shelf (Fig. 8). These sediments have a grand mean of 3.33 phi, slightly smaller than Group 2, and an excess of coarse tail (SK =-0.22).

Two outliers, PC-3 and PC-9, have distributions bearing little or no resemblance to others in the data set (Fig. 18a). PC-3 is the

Figure 18. a) Dendrogram based upon weighted pair group analysis single-linkage of core top sample grain-size distributions (routine after Davis, 1973). The greater the value of sample linkages on the dendrogram axis, the higher the similarity between linked samples. Patterns refer to sample groupings discussed in text.

b) Discriminant analysis of dendrogram groupings (BMDP 7M routine of Jennrich and Sampson, 1982). Projection of Kahe Point core top, grain-size distributions onto a plane determined by the first two canonical variables. Sample code assigned according to the classification determined in (a). Coefficients for canonical variables listed in Table 1.

A)

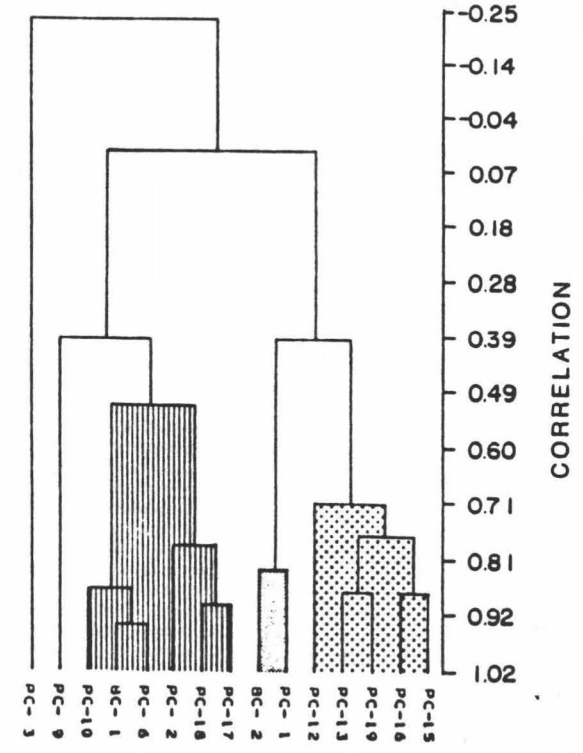

GROUP 1 (Pattern C)

GROUP 2 (Pattern B)

GROUP 3 (Pattern A)

B)

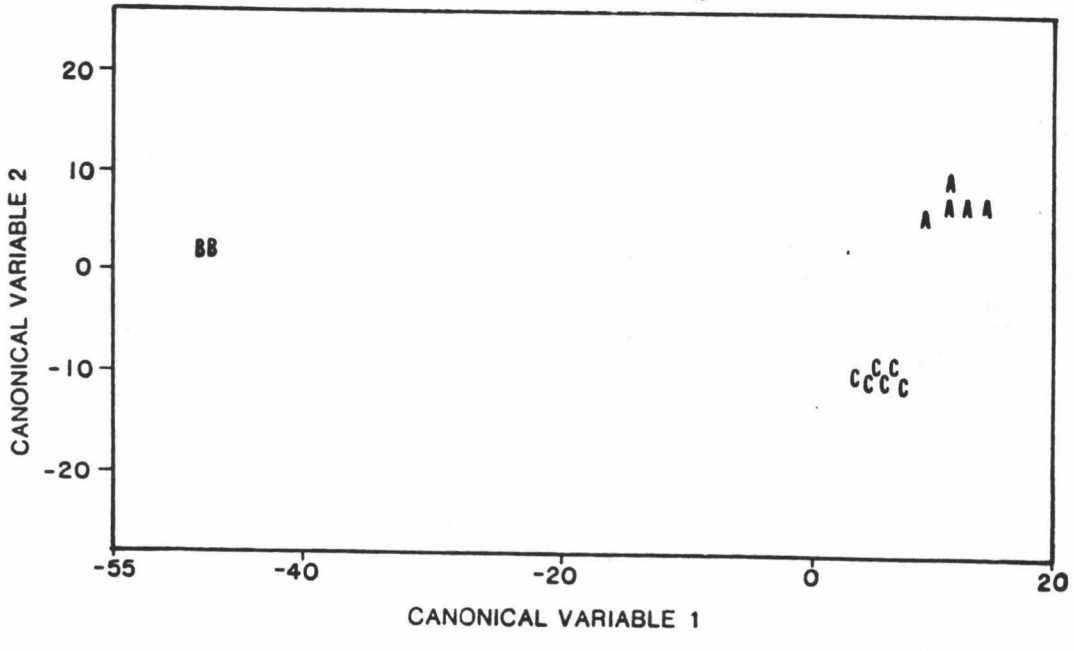

coarsest of all cores and was collected from an area where Pattern B grades into an adjoining boulder zone (Fig. 8). The SeaMARC II image is degraded at the location of PC-9, where the image is lost beneath the ship track. Despite this uncertainty, the interpretation of the image indicates that the core is from Pattern C (Figs. 7 and 8). PC-9 is somewhat coarser than samples in Group 1 and for that reason is set aside on a peripheral branch (Fig. 18a). With the exception of the two outliers, the groupings correspond to the SeaMARC II patterns exhibited by their areas of collection (Figs. 7 and 8).

The distinctiveness of the clusters was examined by discriminant analysis (Pirkle et al., 1984), a procedure which maximizes the distance between group means (centroids, Table 5). Sample positions are projected onto the plane determined by two discriminant function lines (canonical variables). A clear segregation of groupings on the canonical plot indicates that each group determined by cluster analysis is distinctive. The BMDP 7M routine is a stepwise procedure, and in this instance utilized 5 of the 20 variables available for the discriminant equation (Table 6 and Fig. 18b). Sample positions on the plot are determined by the weighted linear combination of percentages in the five selected phi units, each multiplied by its respective coefficient (Fig. 18b). The first canonical variable contrasts the variable -2.0 and the second shows both -2.0 and 0.0 phi as important (Table 6). The three clusters of core-top grain-size distributions plot in widely separated areas of the graph.

Table 5

Mean Grain-size Distributions for Clustered Kahe Point Core-top Samples

Variable*	Pattern C**	Pattern B**	Pattern A**	All Groups**
-2.0	0.0	0.0	0.6	0.2
-1.5	0.0	1.0	0.3	0.3
-1.0	0.0	1.0	0.6	0.4
-0.5	0.0	1.3	1.4	0.7
0.0	0.0	1.8	1.5	0.9
1.0	0.2	11.3	3.0	3.0
1.5	0.4	19.3	3.2	4.4
2.0	1.2	27.3	6.7	7.3
2.5	2.7	12.3	13.6	8.4
3.0	8.3	7.8	23.8	14.2
3.5	15.3	3.3	24.1	16.8
4.0	13.4	8.0	12.3	12.2
4.5	11.9	0.0	3.5	6.9
5.0	17.4	0.0	1.4	8.6
5.5	6.4	0.0	0.4	3.1
6.0	4.1	0.0	0.8	2.2
7.0	4.8	0.0	0.3	2.3
8.0	13.6	0.0	0.0	6.3

* Grain-size in phi units
** Weight percent

Table 6
Coefficients for Canonical Variables
Discriminant Analysis of Kahe Point
Core-top Grain-size Distributions

Variable*	Canonical Variable 1**	Canonical Variable 2***
-2.0	9.04286	-3.55175
0.0	-1.78284	0.41305
1.5	-1.55785	-0.35755
3.0	-0.06702	-0.27398
3.5	-0.00918	-0.25990

*Grain-size in phi units
**X-axis of plot
***Y-axis of plot

DISCUSSION

Sedimentation seaward of the base of the escarpment consists predominantly of hemipelagic settling of silt and clay interrupted by the deposition of shelf-derived sands and gravels. The deposition of these coarser sediments is probably rapid and generated by extreme events such as Hurricane Iwa.

Each of the three clusters of core-top sediments corresponds to a different pattern displayed in the SeaMARC II mosaic (Figs. 7, 8 and 18a). Most of the study area represented by Pattern C (Group 1 cores) is covered by thick sequences of clay and silt. In addition to having similar core-top samples, Group 1 cores all possess a relatively thick upper sequence of fine-grained sediment overlying coarse-grained layers (Fig. 14). The thickness of this upper layer of moderately well sorted, medium to fine silt ranges from 200 to 380 cm with an average of 300 cm. Samples have near-symmetric grain-size distributions (SK=0). Microscopic examination shows that these sediments are composed mainly of planktonic and small, deep benthic foraminifera and fine calcite detritus. As expected, clay minerals are present only in almost undetectable quantities in these fine-grained sediments because the arid Waianae coast produces little run-off. The homogeneity and lack of structure exhibited by these hemipelagic accumulations suggest that constant settling is probably the most prevalent depositional mechanism occurring within the entire study area.

The distributions of Patterns A and B cross the bathymetric contours and converge downslope from the escarpment base, interrupting areas exhibiting Pattern C (Figs. 7 and 8). The orientation of Patterns A and B, the sharpness of their boundaries with Pattern C and the coarse-grained sediments contained in Group 2 and 3 cores collected from these areas suggest that these patterns represent differing types of downslope sediment movement.

Two pieces of evidence suggest that sediments represented by Pattern A originate from the shelf sand wedges. Cores PC-15, -16 and -19 were collected from depths ranging from 460 m to 880 m and yet contain high percentages of shallow benthic foraminifera throughout the entire interval cored at each location (Fig. 16 and Table 4). Most benthic foraminifera display preferred depths of occurrence (Phleger, 1960; Haq and Boersma, 1977) and depth zonations have been compiled for key species around Hawaii (Chave, in press). The appearance or marked increase of shallow benthic species in deeper environments may indicate downslope transport (Phleger, 1960) and different distributions have been used to characterize depositional environments in other Hawaiian offshore zones (Campbell and Erlandson, 1979). High relative percentages of shallow benthic foraminifera (Fig. 16) suggest that the Group 3 sediments are displaced from shallower areas. This suggestion is reinforced by results of the cluster analysis. PC-12 and -13 were collected from the sand wedges located on the shelf, but cluster with the cores collected from Pattern A areas below the escarpment (Figs. 8 and 18a). Both the foraminiferal and statistical associations suggest a genetic relationship between the shelf sediments and those sediments making up Pattern A. The reports from HECO monitoring of significant

losses of sand from shallow areas provide peripheral evidence for this relationship, and suggest by-passing of sand from the shallow shelf areas to the lower slopes.

Most of the cable breaks and sections of buried cable were located directly in the path of the largest swath of Pattern A and marked the path of rapid downslope movement of sediment during the passage of the hurricane. The overlap of these Pattern A swaths reveals multiple paths of sediment movement (Figs. 7 and 17). The largest example of Pattern A exhibits an approximate areal extent of 2.5 km^2. The lengths of cores collected within Pattern A (Fig. 16) indicate a minimum thickness of 2.5 m for these deposits.

The temporal evidence provided by events associated with Hurricane Iwa suggest that Group 2 (Pattern B) sediments were emplaced by rapid movement. Displaced instrument arrays were originally deployed off Kahe Point in a line roughly perpendicular to the coast. Three arrays were moored below the escarpment on seafloor now represented by Pattern B--the SeaMARC II mosaic was obtained after the passage of Hurricane Iwa. Another three arrays were located directly above, on a thick sand wedge on the shelf (Fig. 17). Four of the six arrays moved along a path aligned with a large Pattern B "braid", and the other two were never found. All instruments originally deployed along this line moved at the time of Hurricane Iwa, irrespective of their location on the shelf or slope. Conversely, a nearby array (#1 on on Fig. 17 and Table 2) located on seafloor exhibiting Pattern C, recorded slight increases of near-bottom current velocities, but remained in place during passage of the hurricane. The coarse sediment found in the Pattern B areas, the correlation between the trend of these braids and the paths of

instrument array movement and the proximity to the thick shelf sand wedges demonstrate that Pattern B represents paths of transport and deposition for sediments displaced from the shelf.

The core-top grain-size distributions and the acoustic images provide clues as to the mechanism of deposition. Positive skewness for Pattern B cores (Table 3) indicates distributions with tails toward the fine grain-sizes (large phi values). Excess fines, coarse mean grain-size, and positive surface relief are characteristic of debris flow (Middleton and Hampton 1973). All these properties are attributes of Pattern B sediment.

Although the evidence indicates that rapid sediment movements occur within the study area, only general estimates of recurrence intervals can be made. Hurricane Iwa was reconstructed using a model for a 100-year hurricane event (Noda, 1983). Episodes of unusual hurricane generation are associated with El Niño years (Noda, 1983) and Hurricane Iwa occurred during the intense El Niño of 1982. The linkage of storm occurrence to sediment movement observed off Kahe Point implies that large swaths of seafloor are likely to move at least as frequently as the hurricane recurrence interval, whether this is a 100-year statistical event or a 5 to 7 year El Niño event. The possibility exists that this interval is even shorter; other extreme events such as a major earthquake might also trigger rapid sediment movement.

An additional concern is the spatial permanence of the sediment movement patterns. The surface configurations indicate that paths of sediment movement are influenced by steepness and shape of the escarpment and location of sediment wedges on the shelf (Fig. 19). The

broad swaths of Pattern A (Fig. 8) spread downslope with no corresponding bathymetric relief (Fig. 10). Absence of channels, levees and lobes indicate that Pattern A flow occurs as rapid, unconstrained, individual events in which sediment pours down steep slopes and accumulates on the lower slope areas in thin, overlapping layers (Fig. 19). The suggested genetic relationship between these sediments and those on the shelf areas indicate that Pattern A flow may be confined to areas seaward of large shelf sediment deposits and steep escarpment angles.

The narrow configurations demonstrated by Pattern B and the coincident inflections on bathymetric contours at first appear to indicate that Pattern B represents channelized flow. However, the SeaMARC II images of these features exhibit positive relief (Fig. 7), a characteristic of debris flow (Middleton and Hampton, 1973). The anastomosing configurations on the images suggest that these sediment movements overlap, possibly producing downslope, linear high and low relief which may resemble channel structures on bathymetry (Fig. 19). The anastomosing configurations of Pattern B and their location seaward of thick shelf sand wedges suggest that debris flow may be a common occurrence at any position within the study area located downslope from sources of sediment.

Although slow, constant hemipelagic sedimentation indicated by the thick upper layers of Group 1 cores prevails both volumetrically and spatially (Figs. 8 and 14), the coarse, underlying layers demonstrate that the areas of Pattern C also experience rapid, episodic deposition. The sharp lower boundaries, extremely rapid increases in grain size and percentage of shallow benthic foraminifera and fining-upwards sequences

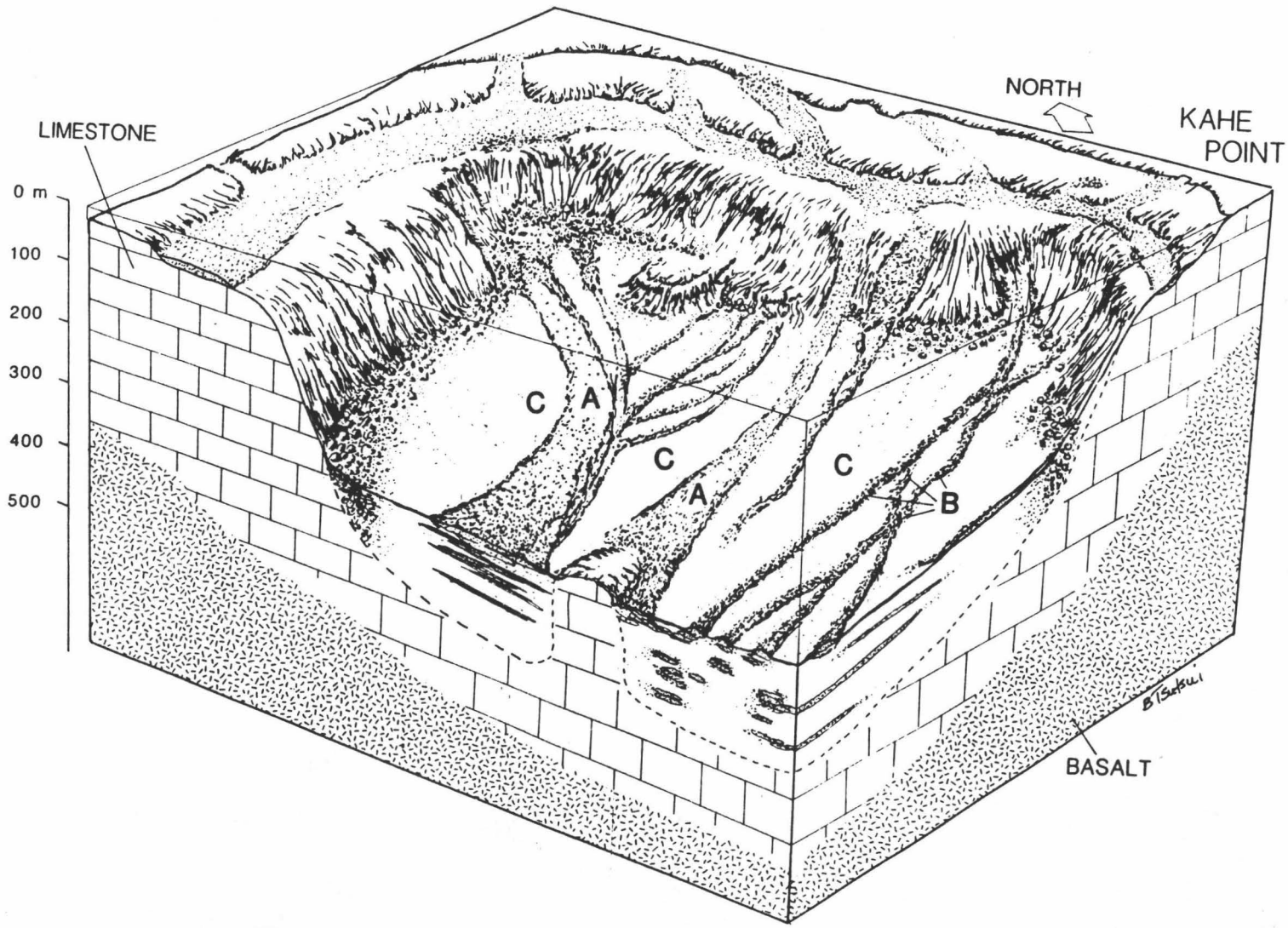

Figure 19. Block diagram showing a general interpretation of vertical pattern of sedimentation for the lower slope areas. Diagram vertical exaggeration approximately 4:1.

found in the coarse layers of PC-17 and PC-18 are all indicative of rapid deposition of displaced sediment. The evidence indicates that the areas represented by Pattern C did not experience slope failure during the hurricane and are stable. In contrast, the events of Hurricane Iwa demonstrate that episodic movement in the area involves transport from the shelf, down the escarpment and across the lower slope rather than failure of the lower slope sediments alone.

CONCLUSIONS

Evidence from SeaMARC II side-scan sonar surveys, ocean bottom photographs and sediment samples indicate a complex submarine geomorphology for the seafloor off Kahe Point. Thick sequences of silt and clay deposited by hemipelagic settling cover most of the lower slope. This sediment cover is interrupted by two differing patterns of downslope sediment movement, manifesting themselves in either broad swaths or long, narrow braids. Vertical sequences of sediment collected from the locations of these patterns contain high percentages of shallow benthic foraminifera, suggestive of displacement from large, thick sand wedges located on the shelf.

Movements of instrument arrays and damage to underwater telephone cables located within this area occurred during the passage of Hurricane Iwa in 1982. Evidence suggests that these events were due to the sediment movements. Paths of sediment movement and their proximity to locations of large, thick sand wedges on the shelf demonstrate that areas downslope of the larger wedges are prone to rapid deposition. Sediment movements affect areas as large as 2 to 2.5 square km and may involve as much as 5 km^3 of sediment.

Although slopes covered by fine-grained sediments represented by Pattern C are generally stable, they are subject to rapid deposition of sediment originating from the shelf. Evidence acquired as a result of Hurricane Iwa shows that recurrence of sediment movements may pose potential hazards to the OTEC cold-water intake-pipe, which will be placed on the lower slope.

Armed only with the knowledge presently available, the safest alternative would be to route the cold-water intake-pipe outside of the re-entrant. However, increased knowledge of the area may make it possible to avoid such monumental measures and to retain a reasonably low risk level. A survey of the shelf area is necessary in order to pinpoint those sand wedges posing the most potential for triggering downslope sediment movement. Secondly, the patterns and direction of sediment movement along the shelf should be studied in order to determine accumulation rates for the sand wedges. Third, additional surveys of the lower slope area should be carried out, with an emphasis on detecting the thickness of sediment cover. This knowledge is essential for locating pipe footing on stable lower slope substrate. The present knowledge of the area indicates that Pattern C areas away from the thicker shelf sand wedges probably provide the most suitable routes.

TABLE 7

Grain-size Parameters for Kahe Point Core Samples*

Core Location Numbers	Mode**	Mean**	Standard Deviation**	Skewness
PC-01-000	2.25	2.26	0.41	0.41
PC-02-000	5.25	4.85	0.43	-0.48
PC-03-000	0.25	0.42	0.64	0.23
PC-06-000	7.25	6.24	0.73	0.06
PC-09-000	6.25	5.42	0.62	0.07
PC-10-000	7.25	6.17	0.79	0.04
PC-12-000	3.75	2.99	0.77	-0.28
PC-13-000	3.25	3.01	0.65	-0.65
BC-01-000	7.25	6.17	0.77	-0.02
BC-02-000	2.25	2.17	0.63	-0.17
PC-15-000	3.75	3.76	0.33	-0.19
PC-16-000	3.75	3.60	0.38	-0.44
PC-17-000	5.25	5.03	0.57	0.09
PC-18-000	5.25	5.10	0.60	0.11
PC-19-000	3.24	3.27	0.36	0.48
PC-15-050	1.75	1.59	0.34	0.15
PC-15-060	0.75	0.81	0.53	0.19
PC-15-068	-1.75	-0.53	0.80	0.60
PC-15-100	0.75	0.80	0.61	0.32
PC-15-150	-1.75	-0.72	0.81	0.25
PC-15-250	-1.75	-0.62	0.95	0.19
PC-16-050	0.75	0.68	0.54	0.21
PC-16-100	0.75	0.83	0.57	0.03
PC-16-150	0.75	0.69	0.55	0.22
PC-16-195	2.25	1.93	0.66	-0.21
PC-17-050	4.75	4.78	0.62	0.07
PC-17-100	5.25	5.19	0.55	-0.14
PC-17-150	4.75	4.77	0.58	0.03
PC-17-200	4.75	4.98	0.63	0.02
PC-17-250	4.75	4.86	0.61	0.08
PC-17-303	4.75	4.52	0.87	-0.41
PC-17-308	6.75	6.11	0.60	-0.19
PC-17-334	4.75	4.53	0.37	0.13
PC-17-350	4.75	4.33	0.36	-0.28
PC-17-360	3.75	3.87	0.50	0.20
PC-17-380	3.75	3.68	0.57	0.49
PC-17-390	3.75	3.74	0.42	0.75
PC-17-400	2.25	2.30	0.64	0.15
PC-17-404	0.75	1.03	0.89	0.47

/continued...

Table 7 (Continued) Grain-size Parameters for Kahe Point Core Samples

Core Location Numbers*	Mode**	Mean**	Standard Deviation**	Skewness
PC-17-444	3.75	3.68	0.76	-0.20
PC-17-450	0.75	1.22	0.90	0.58
PC-18-100	3.75	4.31	0.64	0.03
PC-18-150	3.75	4.37	0.65	0.10
PC-18-200	5.25	5.09	0.46	-0.09
PC-18-250	4.75	4.89	0.61	-0.19
PC-18-300	3.75	3.73	0.62	0.38
PC-18-332	1.25	2.35	0.78	0.10
PC-18-338	4.75	4.12	0.96	-0.16
PC-18-346	3.75	3.88	0.52	0.27
PC-18-355	0.75	1.06	1.12	0.29
PC-18-366	3.75	3.58	0.87	-0.25
PC-18-375	5.25	5.23	0.63	-0.19
PC-18-401	5.75	5.58	0.64	-0.26
PC-18-450	4.75	4.81	0.75	-0.39
PC-18-500	5.25	4.77	0.96	-0.43
PC-18-550	4.75	4.51	0.76	-0.10
PC-19-006	2.75	2.95	0.33	0.90
PC-19-050	1.25	1.51	0.63	1.08
PC-19-100	0.75	0.93	0.62	0.50
PC-19-195	1.75	1.50	0.67	0.24

* Locations shown on Figure 8
** Phi units

BIBLIOGRAPHY

Blackinton, J.G., Hussong, D.M. and Kosalos, J.G., 1983. First results from a combination side-scan sonar and sea floor mapping system (SeaMARC II).In: Proc. 15th Ann. Ocean Tech. Conf., OTS, Houston, TX., pp. 1-5.

Bretschneider, C.L., 1980. Hurricane Fields and Cross-sections: Surface Winds and Currents, Significant Waves and Wave Spectra for Potential OTEC sites. James K.K. Look Laboratory of Oceanographic Engineering, University of Hawaii report 80-1, June, 80 pp.

Brock, V.E. and Chamberlain, T.C., 1967. A geological and ecologic reconnaissance off western Oahu, Hawaii. Pacific Science, 22:373-394.

Brylawski, E., 1984. 40 MW OTEC Pilot Plant Phase 2 Preliminary Design, Offshore Geotechnical Soil Investigation, Oahu, Hawaii. Report for R.J. Brown and Assoc. Inc., Houston, TX., 19 pp.

Campbell, J.F., Coulbourn, W.T. and Moberly, R. Jr., 1970. Reconnaissance Sand Inventory Off Leeward Oahu, Hawaii. Hawaii Inst. Geophys., Tech. Rep., HIG 72-70, 30 pp.

Campbell, J.F. and Erlandson, D., 1979. OTEC-1 Anchor Site Survey. Hawaii Inst. Geophys., Tech. Rep., HIG 79-6, 55 pp.

Chave, E., 1985, in press. Common Living Benthic Foraminifera in Mālama Bay, Hawai'i, with Description of Two New Species. B.P. Bishop Museum Press Occasional Papers, Honolulu, Hawaii.

Chiu, A.N.L., Escalante, L.E., Mitchell, J.K., Perry, D.C., Schroeder, T.A. and Walton, T., 1983. Hurricane Iwa, Hawaii, November 23, 1982. National Academy Press, Wash., D.C., 68 pp.

Coles, S.L., 1979. Annual Report. Kahe Generating Station, NPDES Monitoring Program, Vol. 1. Haw. Elec. Co., Honolulu, Hawaii, 263 pp.

Coles, S.L., 1982. A Visual Reconnaissance of the Bottom Between 20 and 365 m Depth Offshore of Kahe Point, Oahu for the Purpose of OTEC Cable and Pipeline Routing. Haw. Elec. Co., Honolulu, Hawaii, 15 pp.

Coles, S.L., 1984. Annual Report. Kahe Generating Station, NPDES Monitoring Program. Haw. Elec. Co., Honolulu, Hawaii, 221 pp.

Coulbourn, W.T., Campbell, J.F. and Moberly, R. Jr., 1974. Hawaiian submarine terraces, canyons and Quaternary history evaluated by seismic reflection profiling. Mar. Geol., 17:215-234.

Cushman, J.A., Todd, R. and Post, R.J., 1954. Recent Foraminifera of the Marshall Islands. U.S. Geol. Surv. Prof. Paper 191, 69 pp.

Davis, J.R., 1973. Statistics and Data Analysis in Geology. Wiley and Sons, New York, N.Y., 549 pp.

Dengler, A.T., Wilde, P., Noda, E.K. and Normark, W.R., 1984. Turbidity currents generated by Hurricane Iwa. Geo-Marine Letters, 4:5-11.

Devaney, D.M. and Eldredge R., 1977. Reef and Shore Fauna of Hawaii. B.P. Bishop Museum Special Pub. 64:1, Honolulu, Hawaii, 278 pp.

Folk, R.L., 1980. Petrology of Sedimentary Rocks. Hemphill Pub. Co., Austin, TX., 183 pp.

Fornari, D.J., 1983. Final Report, DSV Turtle Dives Off Kahe Point, Oahu, Hawaii. Offshore Investigations Ltd., Chatham, N.Y., 39 pp.

Fornari, D.J., 1984. Preliminary Report: SeaMARC II Side-scan Sonar Image of the Seafloor Off Kahe Pt., Oahu, Hawaii. Offshore Investigations, Ltd., Chatham, N.Y., 14 pp.

Fornari, D.J. and Campbell, J.F., 1986, in press. Submarine Topography Around Hawaii. U.S. Geol. Surv. Prof. Paper 1350.

Griffiths, J.C., 1967. Scientific Method in Analysis of Sediments. McGraw Hill Book Co., New York, N.Y., 508 pp.

Haq, B.U. and Boersma, A., 1978. Introduction to Marine Micropaleontology. Elsevier Pub. Co., New York, N.Y., 376 pp.

Hollister, C.L., 1984. Cable Failures Off Oahu, Hawaii Caused by Hurricane Iwa. Woods Hole Ocean. Inst. Tech. Rep., WHOI 84-31, 26 pp.

Jennrich, R. and Sampson, P., 1979. Stepwise discriminant analysis. In: Dixon, W.F. and Brown, M.B., (eds.) BMDP Biomedical Computer Programs P-Series. Univ. of Calif. Press, Los Angeles, CA., pp 711-740.

Kennett, J. P. and Srinivasan, M.S., 1983. Neogene Planktonic Foraminifera; A Phylogenetic Atlas. Hutchinson Ross Pub. Co., New York, 265 pp.

Lewis,D.W., 1984. Practical Sedimentology. Hutchinson Ross Pub. Co., New York., 229 pp.

Loeblich, A. and Tappan, H., 1964. Protista 2, Sarcodina, chiefly theocambians and foraminifera. In: Moore, R.C. (ed.) Treatise of Invertebrate Paleontology. Geol. Soc. Am. 1-2:C1-C900.

Macdonald, G.A., Abbott, A.T. and Peterson, F., 1983. Volcanoes in the Sea. Univ. of Hawaii Press, Honolulu, Hawaii, 441 pp.

Maragos, J.E., 1979. O'ahu Coral Reef Inventory. Report for U.S. Army Corps of Eng., Honolulu, Hawaii, 379 pp.

Marine Advisers, Inc. 1964. Analysis of Littoral Processes, Kahe, Oahu. Hawaiian Electric Co., Honolulu, Hawaii, 62 pp.

Middleton, G.V. and Hampton, M.A., 1973. Sediment gravity flows: mechanics of flow and deposition. In: SEPM Pacific Section Short-Course Lecture Notes on Turbidites and Deep-water Sedimentation. SEPM, Tulsa, OK., pp. 1-39.

Moore, J.G., 1964. Giant submarine landslides on the Hawaiian Ridge. In: U.S. Geol. Surv. Prof. Paper 501-D, U.S. Geol. Surv., Menlo Park, CA., pp. D95-D98.

Murray, J.W., 1973. Distribution and Ecology of Living Benthic Foraminifera. Crane, Russak and Co. Inc., New York, N.Y., 251 pp.

Noda, E.K., 1982. Site Selection Bathymetry and Sub-bottom Seismic Surveys in the Nearshore Zone Off Kahe Point, Oahu. Tech. Rep. for the Res. Corp. Univ. Hawaii., Honolulu, Hawaii, 15 pp.

Noda, E.K., 1983. Effects of Hurricane Iwa, November 23, 1982 Offshore of Kahe Point, Oahu. Tech. Rep. for the Res. Corp. Univ. Hawaii, Honolulu, Hawaii, 56 pp.

Normark, W.R., Chase, T.E., Wilde, P., Hampton, C.E., Gutmacher, B., Seekins, A. and Johnson, K.H., 1982. Geological Report for the O'OTEC Site Off Kahe Point, Oahu, Hawaii. U.S. Geol. Surv. Open File Rep., 82-468A, 12 pp.

Phleger, F.B., 1960. Ecology and Distribution of Recent Foraminifera. Johns Hopkins Press, New York, 296 pp.

Pirkle, F.L., Howell, J.A., Wecksung, G.W., Duran, B.S. and Stablein, N.K., 1984. An example of cluster analysis applied to a large geologic data set: aerial radiometric data from Copper Mountain, Wyoming. Math. Geo., 16:479-498.

Resig. J.M., 1969. Paleontological Investigations of Deep Borings on the Ewa Plain, Oahu, Hawaii. Hawaii Inst. Geophys. Tech. Rep. HIG-69-2, 99 pp.

Stearns, H.T., 1935. Geology and Groundwater Resources of the Island of Oahu, Hawaii. Hawaii Div. of Hydrography, Bull. 1, Honolulu, Hawaii, 479 pp.

Stearns, H.T., 1974. Submerged shorelines and shelves in the Hawaiian Islands and a revision of some of the emerged shorelines. Geol.Soc. Am. Bull., 85:795-804.

URS Research Co., 1973. Marine Environment Impact Assessment Report for Hawaiian Electric Co., Kahe Point Facility, Oahu, Hawaii. URS-7220-3, 280 pp.

Yuen, P.C., 1981. Ocean Thermal Energy Conversion: A Review. Haw. Nat. Energy Inst., Univ. of Hawaii, Honolulu, Hawaii, 173 pp.